CHAPTER 6 DINORWIC : AN OPTICAL FIBRE FIELD TRIAL

Although the graded-index fibres made at Southampton had been successfully employed in a laboratory-based data-communications link[1], it was evident that an optical fibre field trial would be necessary to establish the suitability of the fibres to be cabled and installed within a more severe operational environment. A collaborative programme was initiated between Southampton University, Pirelli General Cable Works, and the Central Electricity Research Laboratories (CERL) to design, manufacture and install an experimental optical fibre link within the Dinorwic Power Station, under construction in North Wales. A difficult route was selected for the installation in order to demonstrate the considerable advantages of optical fibre cables compared with conventional metallic - conductor cables.

6.1 The Route and System Requirements

The pumped-storage power station under construction at Dinorwic, North Wales utilises two naturally-occurring lakes to form the upper and lower reservoirs of a hydro-electric power station capable of generating 1300 MW of power to meet peak demands on the CEGB grid network. At times of low demand the station draws in power to pump the water from the lower reservoir to the upper reservoir, about 500 metres above the level of the lower lake. The generating station is to be sited within the mountain which separates the two lakes.

There is a requirement to communicate between the main control room of the generating station and the headworks of the upper reservoir, where valves are sited to control the flow of water through the plant. A cable run for this link has been established and its route is shown in figure 6.1; the total length of the route is about 6 km, and the vertical distance between the terminal points is approximately 500 m. A sectional view of the route is shown in figure 6.2, and it will be noted that the final section of the route runs into the main station via a ventilation shaft and access tunnel. Two conventional power cables and two 37-pair control cables run the full length of the route and are employed primarily to control the valve operation at the upper level.

There may also be a need to transmit video information from a monitoring site at the upper level to the main control room[2]. Since the terrain of the route is very severe, it was considered desirable to eliminate the use of repeaters which would be difficult to power and service. It was therefore decided to employ optical fibres to provide an unrepeated link capable of transmitting video and control signals over the major part of the route. As the system will initially be used for experimental purposes, access to the control room was restricted and it was necessary to terminate the link, at the, lower level, in a cabin situated at the top of the ventilation shaft; future extension of the link into the control room would thus be possible before the station becomes operational in 1982. Hence the optical link covers a 5.3 km section of the total cable run.

The optical fibre link runs alongside the conventional cables through a disused slate quarry in a tortuous manner, and up to the headworks at the upper reservoir. It climbs 300 metres in the first 2 km section, and except for a 500 metre section of troughing is installed in 100 mm diameter PVC duct which is buried under discarded slate fragments. As the quarry faces south, temperatures can rise to 30°C in strong sunlight. The upper 3.3 km section of the route follows more gentle contours along a mountain road, and climbs 200 m over its length. However, as the headworks are 700m above sea-level, temperatures as low as - 15°C can be experienced in winter. A noteworthy feature of the route is the rock and slate composition of the terrain which, having a high electrical resistivity, can cause large rises of earth potential under electrical fault conditions.

At the inception of the project the performance requirements of the link were somewhat indeterminate. It had been established that monochrome video data would be transmitted down the link and that a second channel would be required to transmit control data to the camera unit. The basic requirements of the video system were that an equivalent analogue bandwidth of 5MHz should be available and that the signal to noise ratio (SNR) of the video signal at the receive end should be > 35 dB.

An analysis by Dr. F.M.E. Sladen[3] revealed that it would not be possible to meet these requirements using conventional analogue intensity modulation of an LED source. Although laser sources were available, the problems of bias control and output non-linearity precluded their use in an analogue intensity modulation system. Whilst pulse code modulation (PCM) would overcome the problems of laser non-linearity, the bandwidth requirements would be about 70 MHz and the equipment costs would be considerable. Pulse position modulation (PPM) was finally selected for the video system because it offered a convenient form of analogue modulation which could be employed with lasers to give a high SNR. Also proprietary PPM electro-optic transmitter and receiver modules suitable for video applictions were available at reasonable cost[4]. As the performance analysis of a PPM system is complex (the SNR is a non-linear function of attenuation and bandwidth), it was not possible to establish exact performance specifications for the fibre. However, it was felt that a specification of 5 dB/km attenuation at 850 nm (the PPM system's operating wavelength) and 100 MHz.km bandwidth should suffice for the optical cable, and that an additional loss of 0.5 dB/km would be allowed for jointing. The remote-control data for the camera operation would require a bandwidth of approximately 1 kHz and would be easily achieved using fibre of the above specification.

Although only two fibres were needed for the video and control systems, it was decided to incorporate four fibres into the cable, thereby allowing scope for additional experimentation such as looping of the system to provide single-ended operation over 10.6 km, or evaluation of high bit-rate digital equipment over the two spare channels.

6.2 Fibre Specification and Manufacture

From the system specification it was clear that graded-index multimode fibres would readily satisfy the 100 MHz.km bandwidth requirements. Borosilicate clad, phospho-germanosilicate core, graded-index fibres were therefore selected for the link, and the following specification was laid-down for the fibres:-

Overall fibre diameter	:	125 μm
Core diameter	:	63 μm
Borosilicate cladding thickness	:	4 μm
Effective numerical aperture	:	0.2
Attenuation at 850 nm	<	5 dB/km
Intermodal dispersion at 850 nm	<	3 ns/km

Primary coating	:	silicone rubber
Diameter over primary coating	:	250 μm
Secondary coating	:	Nylon 6
Diameter over secondary coating	:	500 μm

The cross-sectional configuration of the jacketed fibre was thus as shown schematically in figure 6.3. Nylon 6 was selected as the jacketing material because of its excellent performance over a wide temperature range; as the problems of pigmentation had not been solved at that time, the fibres were not colour-coded. Although less than 25 km of cabled fibre was necessary to provide the link, considerably more fibre was manufactured for use not only in the final cable but also in the many cabling trials which preceded the final product. As the fibre configuration was identical to that of the 'standard' graded-index fibre described in earlier chapters, the manufacturing details will not be repeated here, and reference will only be made to the optical characteristics of the fibres in relation to the various cabling processes.

6.3 Cable Design and Manufacture

The essential requirements of an optical fibre cable are that it should (a) protect the fibres from externally applied forces during installation and operation, (b) provide a suitable environment in which the fibre can operate, and (c) maintain the transmission characteristics of the fibres themselves. There are a great many approaches to cable design which satisfy the above requirements. One particularly simple approach is to lay the fibres loosely within an internal cavity in the cable, and to embed strength members within the cable sheath[5]. A more conventional approach involves helically stranding the fibres around a central strength member and then applying a protective sheath over the stranded unit[6]; in this construction the fibres must be detorsioned in stranding and must be cabled on special-purpose machinery having precise speed control and low inertia. The lack of such stranding facilities at Pirelli General dictated the use of the former 'loose sheath' approach.

To choose a cable construction the following points were taken into consideration:

1. The cable would be installed in a severe environment in which site construction work would be continuing for another 2 years.

2. The cable would be subjected to extremes of weather.

3. The installation route was particularly tortuous for drawing cable into ducts.

4. No proof testing was being carried out on the fibres and although in short lengths the fibres exhibited very high strength, in long lengths the strain at failure could be of the order of 0.5%.

It was concluded that a rugged cable structure was necessary and that it should possess the following features:-

1. High strength to elongation ratio (1000 N for 0.3%)
2. High radial stiffness and good impact resistance.
3. Sufficient flexibility to permit drawing into ducts in >1 km lengths.
4. Metallic strength member embedded in sheath to minimise sheath retraction at low temperature.

6.3.1 Preliminary Trials

Cabling trials were undertaken to evaluate a number of cable designs, three of which are shown in figure 6.4, along with the basic four-fibre unit common to each design. To produce the 'polylam' unit, four nylon coated fibres were drawn under light backtension (about 0.5N) into the composite aluminium tube/polyethylene sheath as the sheath was formed. The aluminium tube was produced by longitudinal forming of an aluminium tape approximately 20 mm wide by 100 μm thick; the tape was coated on each side with a copolymer which bonded to the polyethylene sheath during extrusion. The aluminium tape was intended to provide a barrier to moisture diffusing through the sheath, and did not form part of the cable's strength element. The strength members were then applied around the central unit in a second operation.

In the first design a tubular strength member of phosphor-bronze was provided by longitudinally forming a phosphor-bronze tape around the central unit, and seam-welding the tape along its length. A further sheath of polyethylene was then applied over the phosphor-bronze tube. Two distinct problems arose with this design: Firstly the stiffness of the sheath was excessive and it would lead to very high tensions when drawing the cable into duct. Secondly, and more importantly, between the stages of forming the polylam unit and applying the phosphor-bronze sheath, tensile loads on the unit were carried by the fibres and the polylam. In particular, inertial loading during winding and sheathing led to excessive 'snatch' loads and fibre breakage occurred.

Thus, in a 1060 m length of four-fibre cable, one fibre was found to have broken in two places whilst the other fibres remained intact. Nevertheless, encouragement was taken from the results of attenuation measurements on the 3.18 km length formed by concatenating the three intact fibres. The spectral loss characteristics of the length are shown for the full length and for a normalised length of 1 km in figure 6.5. At 850 nm, the attenuation over the whole section was only 12.9 dB, giving a normalised attenuation of 4.04 dB/km including joint losses. Thus over the 5.3 km Dinorwic route an attenuation of only 21.4 dB would be predicted, significantly below the specified value. Reference to the results of attenuation measurements made on the fibres before cabling revealed that the summed loss of the individual lengths was within 0.4 dB of the concatenated cabled lengths; the loose-sheath approach to the cable design thus introduced little or no excess loss provided that the fibres were not fractured during cabling.

The second, and third, cable designs shown in figure 6.4 overcame the problems of cable stiffness by employing flexible elements as the sheath strength member. Two or four steel wires were longitudinally laid within the cable sheath, again in a second operation after forming the central unit. Problems arose however, due to buckling of the wires when the cable was bent in a plane which put one or more of the wires into compression. As these designs did not overcome the problems of intermediate processing without a substantial strength element they were not pursued in great depth. It was clear that to guarantee the integrity of the fibres throughout all stages of cabling, a strength element would have to be introduced in the first cabling operation.

6.3.2 The Dinorwic Cable Design

An elegant solution to the cabling problems was achieved by replacing the aluminium laminate tape with a steel laminate tape which would offer strength to the basic cable unit. By incorporating sufficient metal into the basic unit, it was possible to obviate the need for additional strength members applied in subsequent operations. An illustration of the cable structure is shown in figure 6.6: The four jacketed fibres are enclosed within a composite tube comprising a longitudinally-formed paper tube with overlapped edges and a reinforcing steel tube in a polyethylene oversheath. The 7 mm diameter steel tube is produced by longitudinal forming of a 25 mm wide by 150 μm thick tin-plated steel tape which is polymer-coated on both sides. The edges of the steel tape are overlapped during forming and bonded during extrusion of the oversheath. The cross-sectional area of the tape is sufficient to provide a pulling strength of 1000 N for 0.3% extension and a hoop strength of 2500 N per 100 mm of cable. The bonded combination of steel tape and oversheath provides an effective moisture barrier and also prevents the steel tape kinking upon bending of the cable; a minimum bend radius of 50 mm can be withstood. The internal paper tube prevents any possible damage to the optical fibres from the inwardly facing edge of the steel tape, and acts as a heat barrier during the cable sheathing operation. The overall diameter of the cable is 11 mm and its weight is about 80 kgs per km.

One problem which is associated with the loose-sheath structure is that the back-tensioning of the fibres during cabling causes them to move below the neutral axis of the cable as it is wound onto its take-up drum, figure 6.7. Thus the length of fibre incorporated into the cable can be less than the length of the cable itself; if the neutral axis of the cable lies on diameter 'D', and the internal diameter of the cable cavity is 'd', then the length deficit between fibres and cable can be up to d/D .L, where 'L' is the length of cable. Setting L = 1000m, d = 7mm and D = 1000mm, we see that a deficit of up to 7 metres of fibre may occur in a 1km length. In such a case, unwinding of the cable must be accompanied by either retraction of the fibres into the cable, or tensile strain of 0.7% within the fibres.

This situation is obviously undesirable and has been overcome in the Dinorwic cable by employing a novel, driven fibre input to feed fibre into the cable as it is formed[7]. In this manner the length deficit can be offset, and by feeding fibre at a rate which exceeds the cable linespeed it is possible to incorporate an excess length of fibre, thereby achieving a degree of strain relief within the cable.

6.3.3 Cable Manufacture

The cabling line is shown schematically in figure 6.8 for the manufacture of a 4 fibre cable. Each fibre is drawn from a pay-off stand (1) having a back tensioning force of approximately 0.5 N into a driven haul-off unit (3) in which the fibres are gripped between the soft parallel faces of two moving belts. The fibres are driven into a glass guide-tube which extends from immediately downstream of the haul-off into a forming head (4). The paper strip and steel tape are unwound from reels (5,6) and brought together at the forming head. Firstly the paper tape is longitudinally wrapped into a tube around the guide tube, from which the fibres issue. The steel tape is them formed into an overlapped tube around the paper tube before passing through an extrusion crosshead (7) at which the outer sheath is applied. The tractive force necessary to form the cable is provided by a caterpillar unit (8) from which the cable passes onto the take-up drum.

To control the fibre feeding rate, a line-speed pick-off (2) is taken from the steel tape between the pay-off and the forming head. By adjusting the ratio of fibre drive speed to steel tape speed it is possible to control the amount of excess fibre within the cable. Although the fibres are, for example, only 0.5% longer than the cable, the presence of an excess length can be confirmed by observing the undulating path taken by the fibres within the guide, see figure 6.9. The manufacturing process enables lengths of up to 1600 metres (the maximum length of steel tape currently available) to be manufactured in a single operation at line speeds of up to 40 metres per minute.

6.4 Cable Results

Although visual examination of the fibre entering the tube-forming head is a convenient method for checking that the cabling conditions are correct, quantitative measurement of the amount of excess fibre have been made using a pulse delay technique. The effects of cabling upon the attenuation characteristics of the fibres have also been assessed by full spectral measurements upon a length of cable at each stage of manufacture and after installation within the confines of the Pirelli General factory.

6.4.1 Excess Length Determination by Propagation Delay Measurements

In a paper by Hartog et al[8], it is shown that by measurementof pulse transit-times in an accurately-known length of fibre it is possible to determine the amount of stress present within the fibre. In a similar manner the propagation delay per unit length of fibre can be established by pulse transit time measurement on an accurately-known length of jacketed fibre prior to cabling. By performing the pulse delay measurement on the cabled fibre, the length of cabled fibre can be accurately determined and compared with the known cable length to yield the fibre excess length.

The experimental arrangement for the pulse transit time measurement is shown in figure 6.10. A pulse of less than 0.5 ns fwhm duration is launched from a GaAlAs laser operating at 0.85 μm into the fibre under test, and the pulse transit time is measured using a time delay generator and sampling oscilloscope. A small portion of the input pulse is split off onto an APD to provide a reference pulse, and the output pulse from the fibre is detected by a second APD. The time-delay generator produces a trigger pulse for the laser pulser and a reference synchronising pulse. A second synchronising pulse having an adjustable time delay is combined with the reference synchronising pulse by time division and is used to trigger the sampling scope. The propagation time is determined by observing the incident and output pulse waveforms simultaneously on the oscilloscope and adjusting the delayed trigger such that the rising points of both waveforms are coincident. A delay time resolution of 100 ps can be reproducibly achieved.

The following results were obtained from measurements on a 1542 metre length of Dinorwic cable. The pulse transit times measured in a 4700 metre length of fibre, VD281, before and after jacketing were 23181 ns and 23175 ns respectively; the reduction in transit time due to jacketing indicates a compressive strain of approximately 0.025% within the fibre. The time delay of the jacketed fibre was checked over a period of several days and found to be stable. The fibre was then divided into three equal lengths and cabled along with one other fibre, VD251, into a cable of 1542 metres length. The propagation delay measurements on the cabled fibres and the calculated length of each fibre within the cable was as below:-

Fibre No	Transit-time ns	Transit-time per metre ns	Cabled length of fibre m
VD281 A	7645.5	4.931	1550.5
VD281 B	7646.9	4.931	1550.8
VD281 C	7642.4	4.931	1549.8
VD251	7624.2	4.914	1551.5

The propagation delay figures for the three sections of VD281 are within $\pm$ 3 ns of each other, giving equivalent fibre lengths of 1550.4 $\pm$ 0.5 metres. Although the propagation delay was somewhat less in VD251, when allowance was made for the reduced transit-time per unit length, the computed fibre length was 1551.5 m. Thus, each of the four fibres exceeded the cable length by at least 8 metres, thereby providing strain relief of at least 0.5% within the cable.

It is felt that a 0.5% excess fibre length is near optimal since increasing the excess length gives a higher probability of increased attenuation due to buckling within the cable. For example, backscatter measurement on a length containing more than 1% excess length revealed a localised increase of attenuation in a cabled fibre, as shown in figure 6.11. As no other reasonable explanation could be found, the drop-off in signal at about 425m in the cabled fibre was attributed to fibre buckling. This theory was endorsed when, after unwinding the cable during installation, the fibre was able to move, and the loss returned to its original value.

6.4.2 Attenuation Characteristics of Cabled Fibres

Figure 6.12 shows the spectral attenuation characteristics of a length of fibre at the various stages of manufacture. As might be expected of a loose-sheath cable in which the fibre is free of externally-applied transverse forces, there is insignificant change of attenuation due to cabling. Furthermore, the cable was subsequently installed around the factory site and the spectral attenuation measurement was repeated. Again, the attenuation level remains unchanged over the full spectral range. At 850nm, the attenuation of the installed fibre is 4.05 dB/km, only 0.05 dB/km above that of the as-drawn fibre.

Spectral attenuation measurements on other cables gave similar results, as did spot-wavelength measurements performed using a CW semiconductor laser source and an optical power meter as detector. As it was impractical to perform spectral attenuation measurements in the field, the spot wavelength measurements were performed on each cable prior to despatch to form a reference to which subsequent field measurements could be related. The complete set of attenuation measurements will be summarised in section 6.5.2 where the results after installation are also presented.

6.5 Installation, Jointing and Measurements

6.5.1 Installation and Jointing

Although jointing bays were sited every 250 metres along the route, the entire route was covered in only five cable lengths as shown by sections 1 to 5 in figure 6.2. Cables of approximately 1 km length were successfully installed over the most difficult sections of the route and, subsequently, cables of 1.25 km and 1.5 km were laid in the upper part of the route; a 500 metre length was installed over the final section to complete the link.

The table below lists the fibres used to provide the four channel link, and a cross-section of each fibre is shown in figure 6.13:-

Section	Length metres	Channel Number 1	2	3	4
1	980	VD251	VD269	VD266	VD264
2	1080	VD251	VD269	VD266	VD264
3	1250	VD251	VD244	VD235	VD255
4	1500	VD251	VD281	VD281	VD281
5	500	VD269	VD269	VD272	VD272

Wherever possible core size and NA mismatches between different sections of each channel were minimised by matching the fibres within the cables. Thus in channel 1, 4.8 km of the link is provided by a single fibre, VD251, whilst in the other channels only the first two sections could be perfectly matched. However, from the fibre cross-sections in figure 6.13, it is evident that only minor geometrical mismatch occurs in any channel.

Installation was carried out manually with the cables being drawn in a single 'pull' from one end of the section. It was found that the flexibility of the cable was sufficient to allow the 1500 metre cable length to be drawn through the duct at a maximum pulling tension of only 800 N. Over the inclined troughing section the cable was laid in the trough and subsequently clamped at about 10 metre intervals. Spot-wavelength measurements of attenuation were made on all fibres after installation using the cut-back technique with a CW GaAlAs laser source.

At each jointing section the cable ends were encapsulated in polyurethane resin within the base of a standard BPO Type 31A joint enclosure. Fibre tails were brought through the encapsulant into the ready-access chamber of the enclosure where the fibres were jointed using the BPO copper-substrate V-groove technique[9]. The joints were then secured on a glass substrate and placed within a tray in the joint housing; the tray also provided sufficient room for spare fibre to be coiled, thereby allowing joints to be remade without having to remake the enclosure. Considerable difficulty was experienced in making the joints using the V-groove technique. It was found that a very high dust level in the jointing chambers was leading to misalignment of the fibres within the V-grooves and also to the contamination of the epoxy adhesive which was used to bond the fibres and to index match the joint. Furthermore, the mechanical reliability of the joints was put into doubt when four of the joints were found to have broken under the combined effects of static fatigue and vibration from the heavy vehicles passing the joint bays.

To overcome these problems all joints were subsequently remade using an arc-fusion splicing equipment loaned by Sieverts Kabelwerk, Sweden. The fusion splices not only solved the alignment problems, but also produced a much stronger splice in which the fibres were held straight; tensile loads were carried across the splice by means of a steel split-sleeve clamped to the jacketed fibre on each side of the splice. Each splice was protected by encapsulation in silicone rubber and by the application of a heat-shrink sleeve over the full length of the splice and its steel split-sleeve; no splice failures have occurred over the 10 month period since their installation.

6.5.2 Performance Measurements

Attenuation measurements were performed on the individual cable lengths after installation and also on the completed link after jointing. Using the attenuation results obtained during the various stages of cable manufacture it is possible to follow the evolution of attenuation and to assess the quality of the joints by comparison of the cumulative attenuation figures of each channel with the measured end-to-end attenuation. In Table 6.1 the attenuation level of each fibre section is summarised at the different manufacturing stages, and the predicted cumulative loss is calculated assuming zero joint loss. Particularly noteworthy features of the results are the consistently low attenuation levels obtained in the jacketed and cabled fibres; in no case did the attenuation of a fibre exceed the 5 dB/km specification limit. Thus, the predicted loss values for the concatenated sections fall well below the target figure of 26.5 dB for the installed cable (neglecting allowable joint losses).

Detailed examination of the results show that the values obtained over the final section are generally higher than those obtained elsewhere. This is unlikely to be a consequence of poor fibre and cable manufacturing processes, but more probably results from the measurements being performed on a short length of cable.

Comparison of the predicted cumulative losses with the actual attenuation values measured over the V-groove-jointed link show that the actual values were significantly higher than was expected, see Table 6.2. Possible causes of this discrepancy were (1) additional losses due to fibre mismatch at joints, and (2) high jointing losses due to fibre to fibre misalignment and contamination of the index-matching epoxy.

If the former effect were the dominant factor, then channel 1 would be expected to show the lowest excess loss, since dis similar fibres were spliced only at the joint between sections 4 and 5. In reality, the end-to-end joint loss of channel 1 exceeded the predicted value by 5.9 dB, clearly too much to be attributed to mismatch losses. Furthermore, the mean joint loss over all four channels obtained by subtracting the predicted losses from the actual end-to-end losses amounted to more than 1.2 dB per joint, considerably higher than the specification limit and also much higher than had been experienced in a laboratory environment (see for example figure 6.5). The high joint losses were therefore attributed to the unsuitability of the V-groove splicing technique to field use in dirty environments, and the decision was taken to replace all joints with splices made by arc-fusion welding of the fibres.

The significant improvement in the joint quality after fusion splicing is shown by the attenuation measurements over the fusion spliced link, see Table 6.2. The end-to-end attenuation measurements are much nearer the predicted values, and the mean joint loss of 0.19 dB lies well inside the specified value. Using a backscatter system developed at Pirelli General, it was possible to monitor the quality of the fusion splices as they were made and to remake lossy joints as and when necessary. Prior to removing the V-groove joints from the link it was possible to use the same backscatter equipment to determine the V-groove joint losses over the first three sections of the link. Thus in figure 6.14, the backscatter plots of the first three sections of channel 1 (fibre VD251) are plotted for the V-groove spliced and fusion-spliced conditions. The improvement as a result of fusion splicing is significant, and is particularly highlighted when the results are plotted on a logarithmic scale as in figure 6.14 b. For the two splices shown, the total joint loss dropped from 2.1 dB for the V-groove to only 0.34 dB for the fusion joints, an effective attenuation reduction of 0.5 dB/km over the 3.3 km section shown in the figure. It is also interesting to note the uniformity of the attenuation along the length of the fibres; after fusion splicing the loss of the concatenated section was only 8.5 dB at the measurement wavelength of 904 nm.

In Table 6.3, the attenuation results are summarised in terms of the mean attenuation levels for each channel and for the whole link at each manufacturing stage. Again, the consistency of the results is striking, as is the considerable improvement after fusion splicing. For the jacketed, cabled, and installed fibres the mean attenuation varies by less than 0.1 dB/km about a value of 3.6 dB/km. In the completed link, the additional loss due to fusion splicing amounts to only 0.15 dB/km, giving an attenuation of only 3.77 dB/km for the link as a whole.

The bandwidth performance of the link was determined by pulse dispersion measurements on each channel. A GaAlAs laser operating at 0.85 μm was used as the source, and a silicon avalanche photodiode was used as detector; the semiconductor laser produced a pulse of about 500 ps fwhm width and was operated at a repetition rate of 350 kpps. Light from the laser was launched via a 100 metre launch tail into the fibre under test, and at the far end of the link the output pulses were imaged onto the APD and displayed on a sampling oscilloscope. Because the repetition rate of the laser was high, it was possible to trigger the scope internally, thereby overcoming the problems of providing a delayed trigger pulse. The output pulse waveforms from the four channels and also the output pulse from the 100m launch tail are shown in figure 6.15. All four channels are seen to exhibit very similar pulse dispersion characteristics. Deconvolving the input pulse width from the output waveforms gives the following fwhm pulse dispersion values:-

	Pulse Dispersion	
Channel No.	Total ns	Normalised ns/km
1	4.3	0.8
2	4.2	0.8
3	5.0	0.9
4	5.3	1.0

The normalised results are calculated in terms of the pulse dispersion over a 1 km length assuming a linear length - dependence. Using the theory of Gaussian pulses to transfer the time-domain results into the frequency domain[10], the equivalent analogue bandwidths of channels 1 to 4 are approximately 100 MHz, 100 MHz, 90 MHz and 80 MHz respectively over the full 5.3 km length. As might be expected of a jointed system, the bandwidth x length product of the concatenated fibres exceeds the mean bandwidth x length product of the individual fibres which form the link. Whilst this may in part be due to the effects of jointing over-compensated and under-compensated fibres within the same channel[11], a more likely cause is the mode filtering effect of joints, which reduces the width of the propagating pulse by attenuating higher-order modes at the joints. Nonetheless, the pulse dispersion results indicate that the bandwidth performance of all four channels within the link exceeds the bandwidth requirement of the video system by at least an order of magnitude. Similarly, the measured results lie well within the original specification of 3 ns/km intermodal dispersion for the jointed link.

6.6 System Operation and Performance

Having achieved such excellent results from the attenuation and pulse dispersion measurements on the link, it was decided to install not only the video and control systems but also a high bit-rate digital communications system which would provide a more searching test of the fibres' performance.

6.6.1 Video and Tele-control Systems

A schematic diagram of the video and tele-control equipments is shown in figure 6.16. At the upper reservoir level a monochrome television camera is coupled to an electro-optic transmitter employing pulse position modulation (PPM) to provide a 50 Hz to 5.5 MHz analogue bandwidth. The PPM equipment modulates the position of a 13.3 Mhz carrier pulse to provide analogue transmission using 'digital' pulse techniques[4]. The transmitter employes a pulsed laser source operating at approximately 850 nm, and light from the laser is coupled into the optical fibre channel through a demountable jewelled-ferrule connector. At the lower level of the link, the output pulse from the fibre is detected using a receiver incorporating an APD with automatic bias control and analogue circuitry which converts the 13.3 MHz carrier signal back into an analogue video signal which is displayed on a television monitor. For a 35 dB SNR at the receiver output, the insertion loss of the system could be up to 50 dB. However, when allowance is made for the use of 63 μm core size 0.2 NA fibres, the permissible link loss is reduced to about 40 dB. A further reduction in SNR can result from the effects of pulse dispersion, which increases the risetime of the carrier pulses thereby leading to uncertainty of timing; at low signal levels the timing jitter becomes significant and the system performance is reduced. However, no problems of this nature were anticipated due to the exceptional attenuation and bandwidth capabilities of the optical fibres within the link.

Remote control of the camera functions are provided at the lower level by means of a conventional 15 function tele-control unit interfaced with an electro-optic transmitter. The normal repeated train of fifteen 0.5ms pulses from the control unit, one for each function, is encoded to provide a 1.0ms pulse at each point in the train where a function is required to operate. These 'high' and 'low' pulse levels are then converted to corresponding 1Mb/s and 2Mb/s pulse streams and fed to the transmitter, which also employs a laser operating at 850nm. At the upper reservoir level the incoming pulse train is detected by an APD receiver, and decoded to switch the appropriate control functions.

Very good performance of both systems has been provided during preliminary trials. From the subjective viewpoint, a steady, noise-free video display is obtained and the tele-control operates with precision. Although neither system has yet been thoroughly evaluated, it is evident from the attenuation and dispersion figures for the link that in both cases there is ample margin in hand. In the case of the video system it was demonstrated that 34 dB fibre loss could be tolerated without significant degradation of picture quality. The greatest problem experienced to date has been the stability of the jewelled-ferrules which are fitted to each fibre tail: it has been found that unless great care is taken in bonding the ferrule to the fibre, and also in polishing the fibre end face, additional coupling losses of as much as 10 dB can occur over each channel. However, even when additional losses of this order have occurred, the system margin has been sufficient to maintain satisfactory operation of the equipment.

6.6.2 34 Mb/s Line Terminal

To assess the link's capability to transmit digital telecommunications signals, a 34 Mb/s line terminal was provided by Telettra Spa of Milan, Italy. A detailed description of the equipment and its operational characteristics has been given elsewhere[12] and, as the equipment was employed at Dinorwic as a 'black-box', a description of its internal structure will not be given here. There are, however, some salient features which are worth noting in relation to its operation within an optical fibre system:-

Firstly the equipment is designed to operate with any standardised 34 Mb/s source, and to provide communications capacity equivalent to 480 telephone channels. Although the incoming bit-stream will have a bit-rate of 34.368 Mb/s, to meet the need for a binary optical line-code with timing recovery at the receiver, the output line-rate is actually 41.242 Mb/s.

Secondly, the system is designed for use with graded-index multimode fibres over section lengths of the order of 5 km. An LED source operating at 904 nm and an APD receiver are employed and give a system attenuation margin of about 25 dB for a bit error rate (BER) of better than 1 in 10^9.However, because the LED source has a 40 nm linewidth, the system performance over lengths in excess of 5 km is generally limited by material dispersion rather than attenuation. Although much longer repeater section lengths could be envisaged with the use of a laser source, it is felt that the greater reliability of the LED is the more important consideration at present.

As only one system was provided it was necessary to operate the equipment in a single-ended mode with both the transmitter and receiver sited within the cabin at the lower level of the link. This also facilitated the evaluation of the equipment by measurement of the BER over prolonged periods. From the system's optical power budget it was obvious that it would not be possible to operate over the 10.6 km loop provided by jointing the two spare channels at the upper reservoir level; a suitable loop could only be provided by looping the two spare channels at one of the joint bays along the route. Thus, by looping the fibres at the third jointing position a 6.6 km link was obtained which it was hoped would provide a demanding test of both fibre and system.

Hence, channels 1 and 2 were broken at the third jointing position and looped back using a fusion splice. The attenuation of the loop, measured using the cut-back method with a 904 nm LED source, was 22.7 dB (3.44 dB/km). Although measurements with a laser source were somewhat lower (21.2 dB) the LED measurement is more representative of the operating conditions of the Telettra equipment.

The pulse dispersion around the loop was measured using the pulsed laser system used in the previous dispersion measurements. As with the four 5.3km channels, the pulse dispersion around the loop was very low, as shown in figure 6.17; the 300 ps fwhm input pulse had broadened to a 5.8 ns fwhm pulse at the end of the 6.6km loop. Using the results of Payne and Hartog[13] for the material dispersion within the fibres, it is possible to deconvolve the input pulse width and material dispersion component from the output pulse to obtain a value of 5.6ns for the intermodal dispersion over the 6.6km length. As the Telettra equipment operates at about 900nm, material dispersion of approximately 80 ps/nm.km would be expected. Thus for an LED source having a 40 nm linewidth the total pulse broadening would amount to approximately 22ns over the 6.6km link. When this is convolved with the 10ns LED pulsewidth an output pulsewidth of 24ns fwhm would be expected. As the bit period is only 24.2ns considerable 'intersymbol' interference should be observed at the receiver.

The line terminal was linked to a pseudo-random bit generator/error detector (Hewlett Packard Model 3780) and the transmitter and receiver were coupled to the optical fibre loop using demountable connectors. The line attenuation was checked using an optical power meter to detect the output power from the loop; the power coupled into the loop was determined by inserting a short fibre tail at the launch end and measuring the output from the tail. The following results were obtained:-

Measured power into launch tail	=	-20.2 dBm
Measured received power from 6.6 km line	=	-42.7 dBm
Total line loss	=	22.5 dB
	=	3.4 dB/km
Minimum received power for BER of 10^{-9}	=	-45.7 dBm
System margin	=	3.0 dB

The attenuation measured with the line terminal agrees very well with the cut-back measurement given above, and it can be seen that even when operating over 6.6km of fibre, the fibre loss is sufficiently low to leave a 3.0 dB system margin.

The eye-diagram at the APD detector output was monitored using a high-speed real-time scope with FET probes and is shown in figure 6.18, where the horizontal scale corresponds to 5 ns/div. As was expected from the material dispersion calculations above, the fwhm received pulsewidth corresponds almost exactly to the bit period of 24ns, and considerable intersymbol interference is present. However, at the decision point the eye-opening is substantial, and considerable tolerance is available for setting the decision level.

The bit error rate measurements over the link gave similarly satisfying results. Over a four-day test period after commissioning of the terminal a BER of better than 1×10^{-10} was obtained; subsequent checks over a six month period have shown that the system is stable and that BER has been better than 10^{-10} (the limit of the Hewlett Packard equipment). Furthermore, by accumulating the total number of errors and monitoring the number of days for which the equipment has been operational, an equivalent BER of approximately 10^{-12} has been maintained.It is intended to continue monitoring the performance of the link over the next year, and possibly to install a laser transmitter to enable 34 Mb/s operation over the 10.6 km link formed by looping the channels at the upper level. Finally, it should be mentioned that this system represents the first operational 34 Mb/s optical fibre communications link installed within the U.K. Although it is at present transmitting only pseudo-random data it is anticipated that a second terminal may be installed in due course, and that the two systems may be used over the 5.3km route to feed a microwave link at the top of the Dinorwic mountain which will form part of the CEGB's integral communications network.

6.7 Reference to Chapter 6

1. Sladen, F.M.E., and Norman, S.R.: 'Data transmission using optical fibres', Electronic Engineering, June 1977, pp 57-63.

2. Rogers, A.J. : 'Experimental fibre-optical communications link at Dinorwic', CERL Laboratory Note RD/L/N 66/79, CERL, Leatherhead, U.K.

3. Sladen, F.M.E.: 'Fibres for optical communications', Ph.D.Thesis, University of Southampton, Nov, 1978.

4. ITT Electro-Optics Products Division, Leeds, U.K.

5. Slaughter, R.J., Kent, A.H., and Callen, T.R.: 'A duct installation of 2-fibre optical cable', First European Conference on Optical Communications, London 1975, pp 84-86.

6. Grasso, G., Pizzorno, M., and Portinari, A. : 'High quality optical fibre cable for telecommunication',- Proc. 27th IWCS, Washington 1978.

7. European Patent Application No. 80302477.7, 22-7-1980, 'Optical Fibre Cable'.

8. Hartog, A.H., Conduit, A.J., and Payne, D.N.: 'Variation of pulse delay with stress and temperature in jacketed and unjacketed optical fibres', Opt. Quant. Electron., 11 (1979), pp 265-273.

9. Hensel, P.C., North, J.C., and Stewart, J.H.: 'Connecting optical fibres', Electronics and Power 23 (1977), pp 133-135.

10. Midwinter, J.E.: 'Optical Fibre Communications' John Wiley and Sons, New York 1979, p.398.

11. Eve, M., Hartog, A.H., Kashyap, R., and Payne, D.N.: 'Wavelength dependence of light propagation in long fibre links', Proc. Fourth European Conference on Optical Communications, Genoa 1978, pp 58-63.

12. Castelli, R., Mazzuco, R., and Tamburello, M.: 'Design, construction and performance of a 34Mb/s optical fibre transmission system', Proc. Fifth European Conference on Optical Communications, Amsterdam 1979, pp 22.5-1, 22.5-4.

13. Payne, D.N. and Hartog, A.H.: 'Determination of the wavelength of zero material dispersion in optical fibres by pulse-delay measurements', Electron. Lett. 13(1977), pp 627-629.

Table 6.1 Attenuation of Dinorwic fibres throughout cable manufacture and installation.

Channel 1 Attenuation dB/km at 850 nm

Section:	1	2	3	4	5
Jacketed	3.6	3.6	3.6	3.6	3.8
Cabled	3.4	3.9	3.5	3.5	3.8
Installed	3.3	3.4	3.5	3.2	4.3

Predicted cumulative loss $\sum_{i=1}^{5} XiLi$ = 18.2 dB (installed)

Channel 2 Attenuation dB/km at 850 nm

Section	1	2	3	4	5
Jacketed	3.8	3.9	4.1	3.4	4.3
Cabled	3.8	4.4	3.6	3.6	4.0
Installed	4.2	4.1	3.6	3.2	4.3

Predicted cumulative loss = 20.0 dB

Channel 3 Attenuation dB/km at 850 nm

Section	1	2	3	4	5
Jacketed	3.8	4.2	4.1	3.3	3.7
Cabled	4.0	4.5	3.6	3.2	4.0
Installed	4.6	4.0	3.5	3.3	4.3

Predicted cumulative loss = 20.3 dB

Channel 4 Attenuation dB/km at 850 nm

Section	1	2	3	4	5
Jacketed	2.9	2.9	4.0	3.3	4.9
Cabled	2.8	3.2	4.4	3.2	3.3
Installed	2.9	2.8	4.4	3.3	4.3

Predicted cumulative loss = 18.5

Table 6.2 Dinorwic Project: End to end loss measurements on V-groove jointed and fusion-spliced link.

Channel	1	2	3	4
Predicted cumulative loss	18.2	20.0	20.3	18.5
V-groove jointed	24.1	23.6	22.4	26.5
Fusion spliced	19.1	20.7	21.7	18.6

All values are for total end-to-end attenuation measured at 850 nm using cut back technique and laser source.

Table 6.3 Dinorwic Project Comparison of mean attenuation levels at all stages of project.

Channel	1	2	3	4	Mean Value
Jacketed fibre	3.6	3.8	3.8	3.5	3.67
Cabled fibre	3.6	3.8	3.8	3.4	3.65
Installed cable	3.4	3.8	3.8	3.5	3.62
V-groove jointed	4.5	4.4	4.2	5.0	4.52
Fusion spliced	3.6	3.9	4.1	3.5	3.77

All values are for mean attenuation levels in dB/km at 850 nm using cut back technique and laser source.

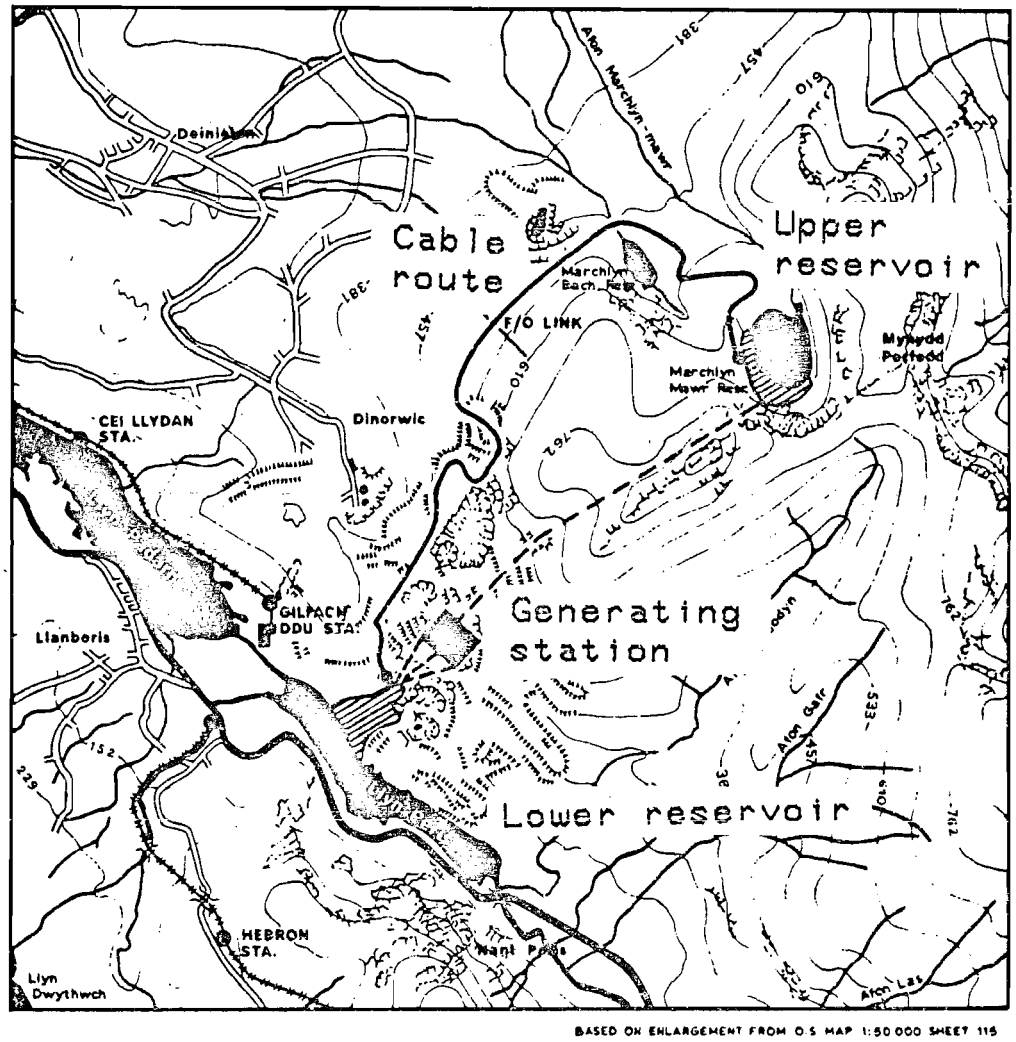

MAP OF DINORWIC PUMPED-STORAGE POWER-STATION

The location of the upper reservoir leads to a difficult and tortuous cable route.

FIGURE 6.1

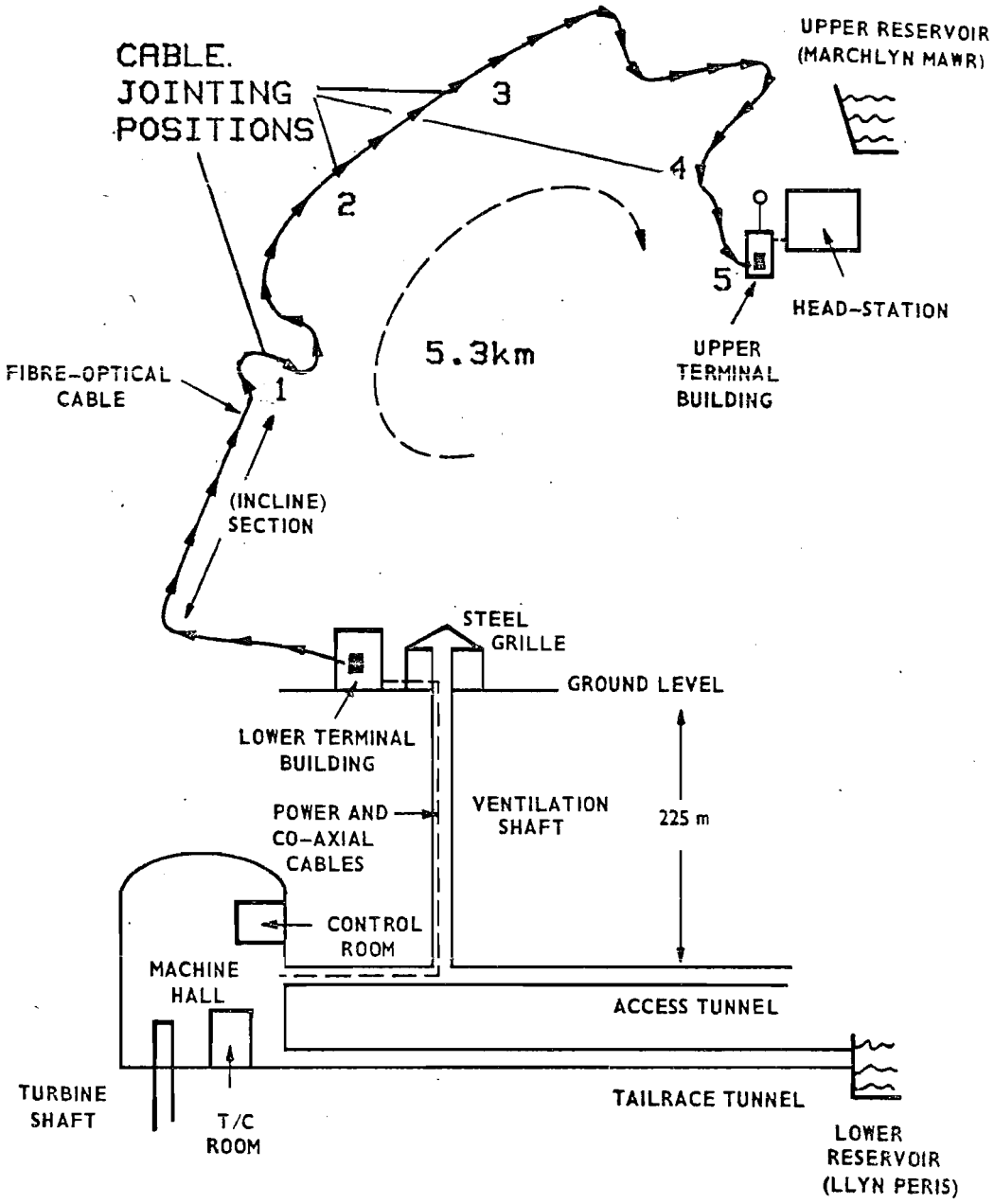

SECTIONAL VIEW OF CABLE ROUTE BETWEEN CONTROL ROOM OF GENERATING STATION AND HEADWORKS OF UPPER RESERVOIR. THE 5.3km SECTION TO BE COVERED BY THE OPTICAL FIBRE CABLE IS ALSO SHOWN.

FIGURE 6.2

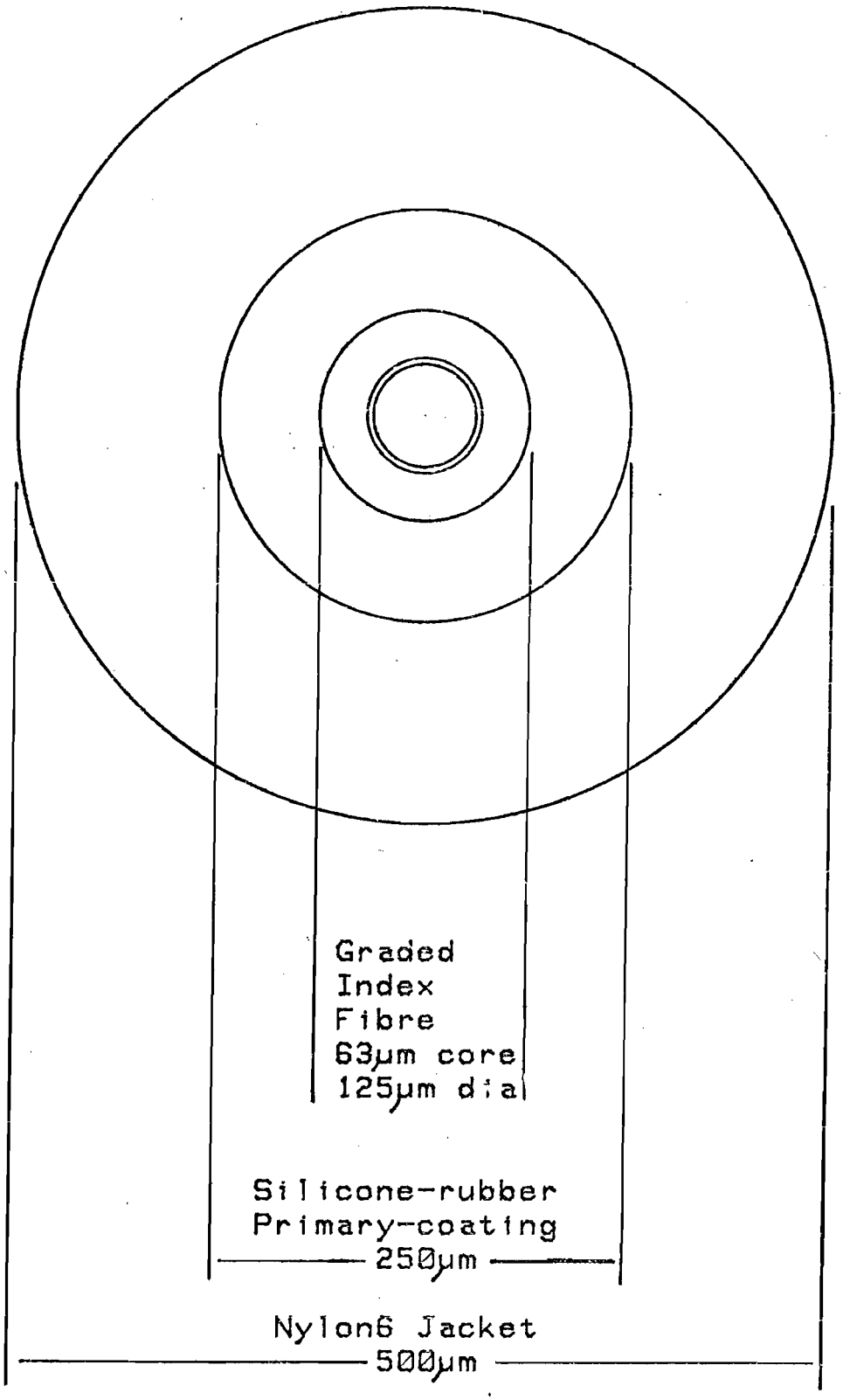

DINORWIC PROJECT: JACKETED FIBRE CONFIGURATION

FIGURE 6.3

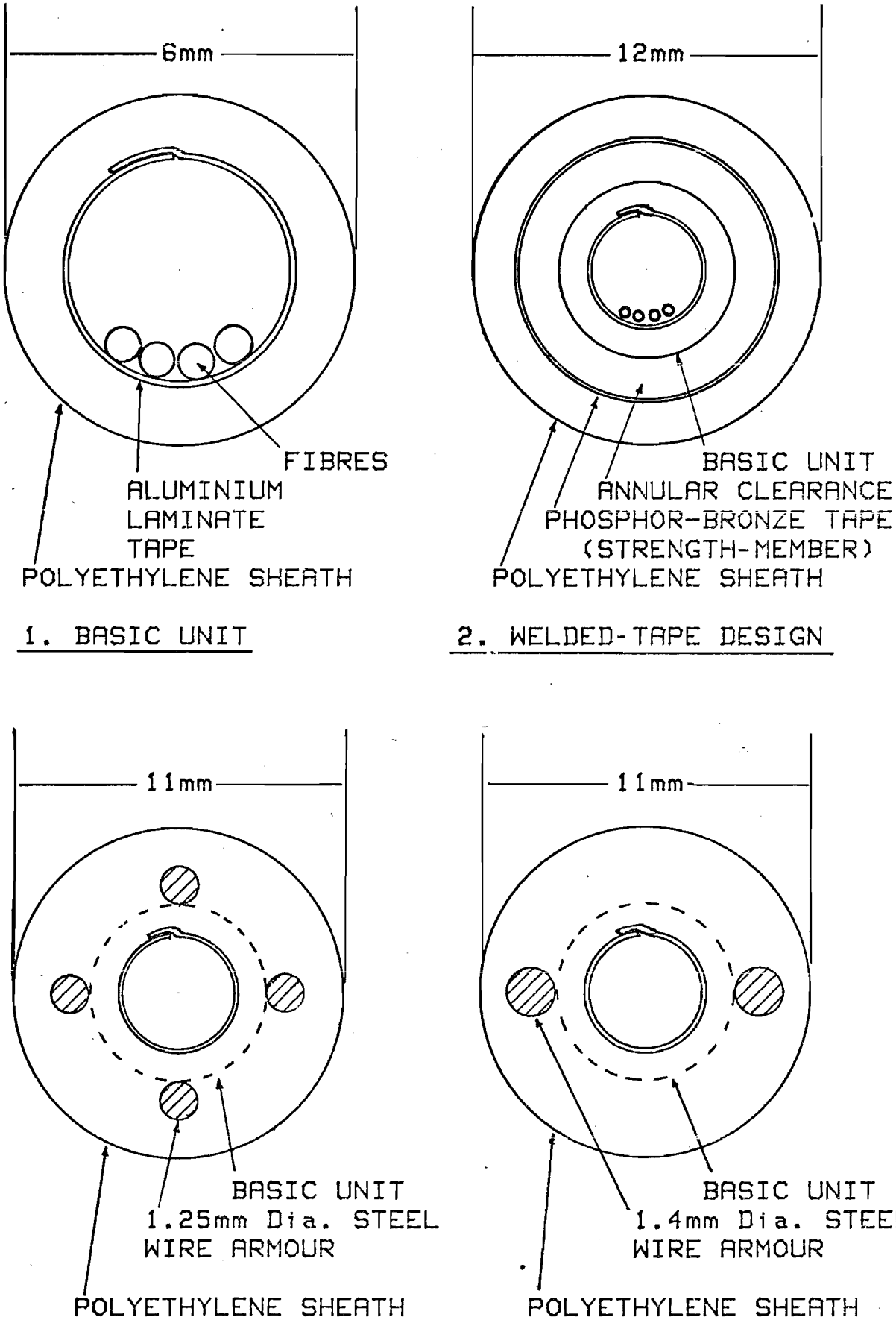

DINORWIC PROJECT: EARLY CABLE DESIGNS

FIGURE 6.4

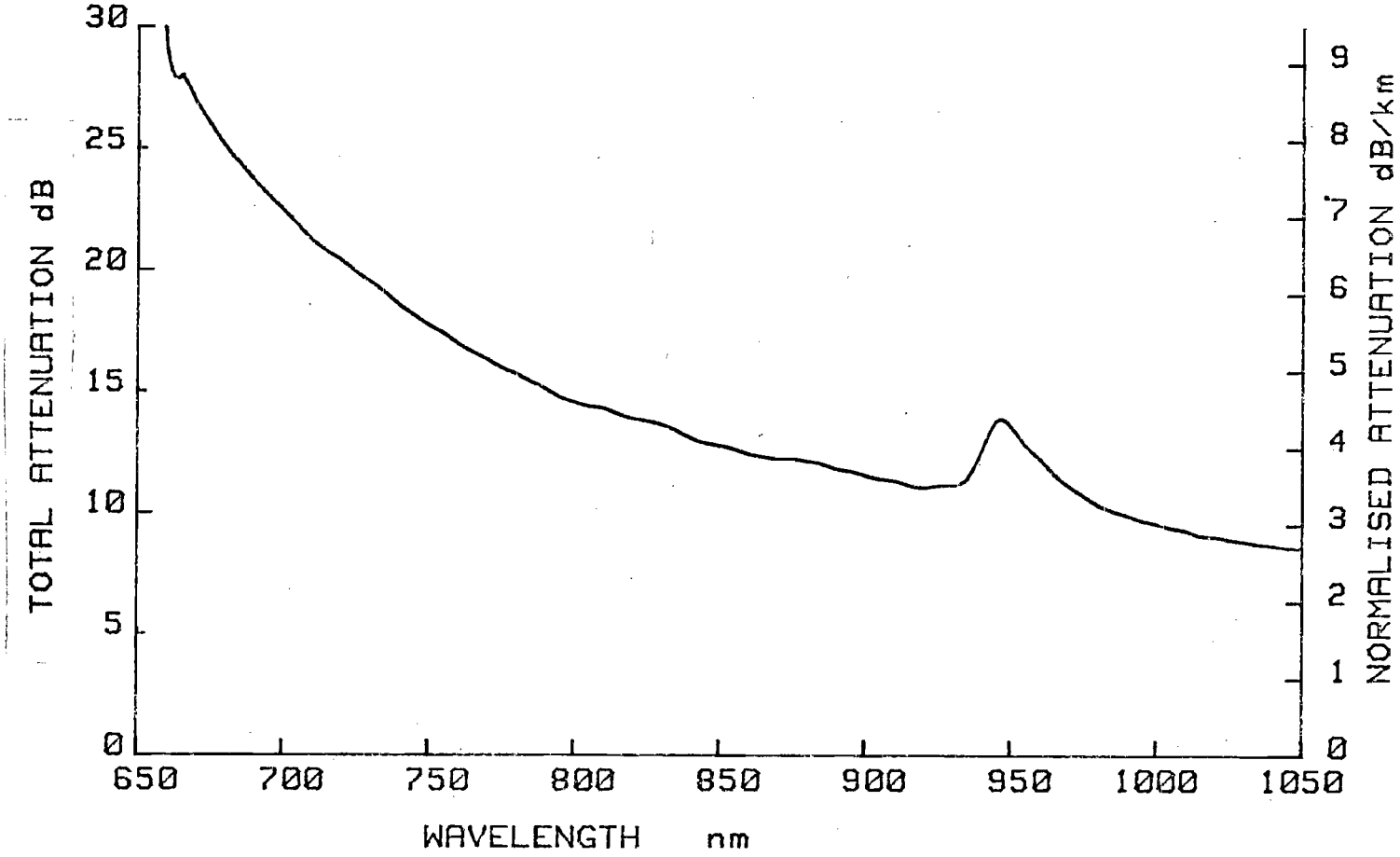

SPECTRAL ATTENUATION OF 3.18km CONCATENATED FIBRE IN 1.06km LENGTH OF PHOSPHOR-BRONZE-SHEATHED LOOSE-TUBE CABLE.

FIGURE 6.5

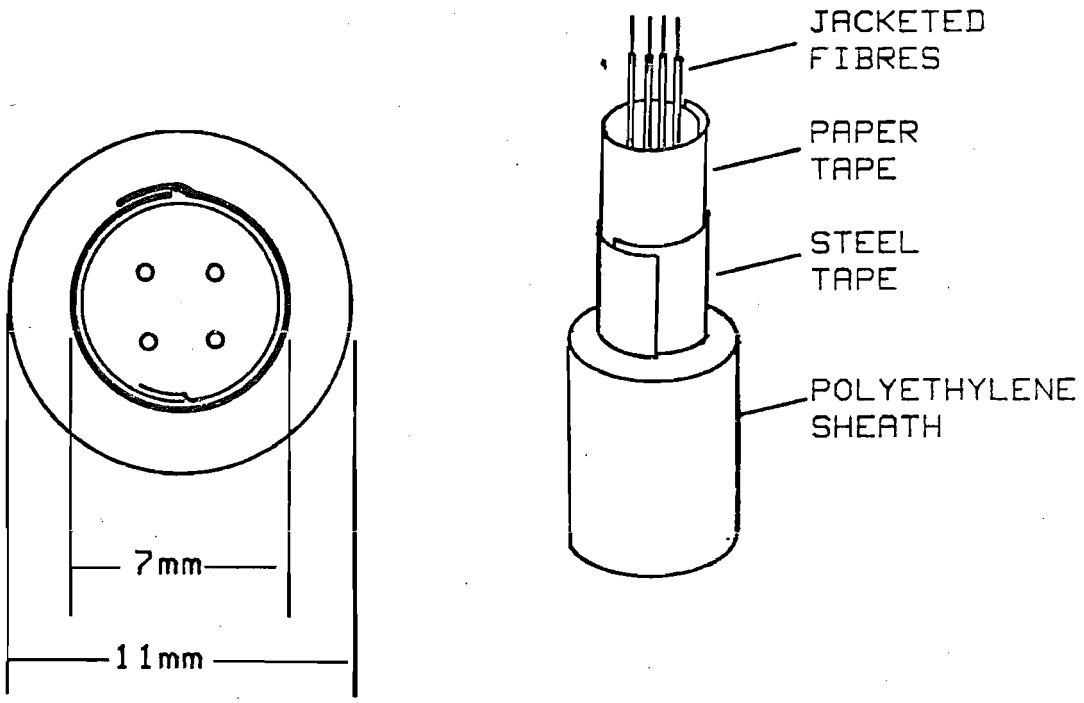

DINORWIC PROJECT: FINAL CABLE DESIGN

FIGURE 6.6

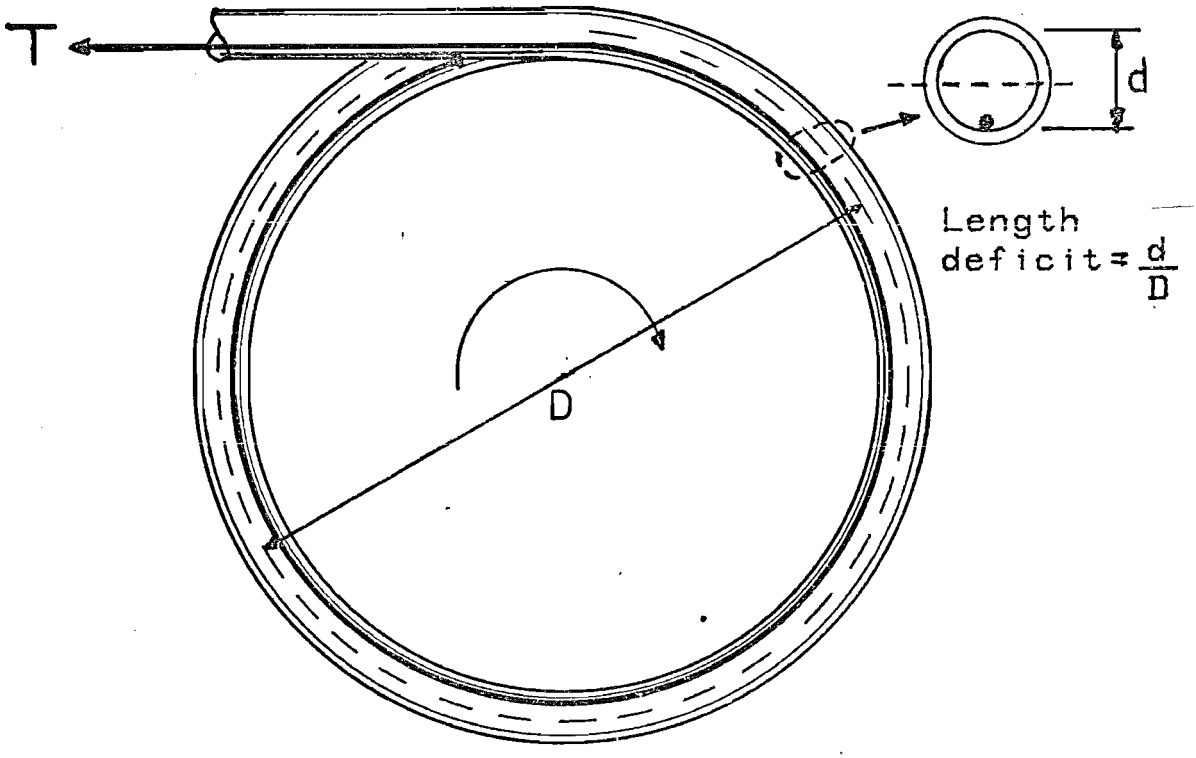

FIBRE LENGTH DEFICIT IN LOOSE-TUBE CABLE
Back-tension, T, pulls the fibre below the neutral-axis of the drummed cable.

FIGURE 6.7

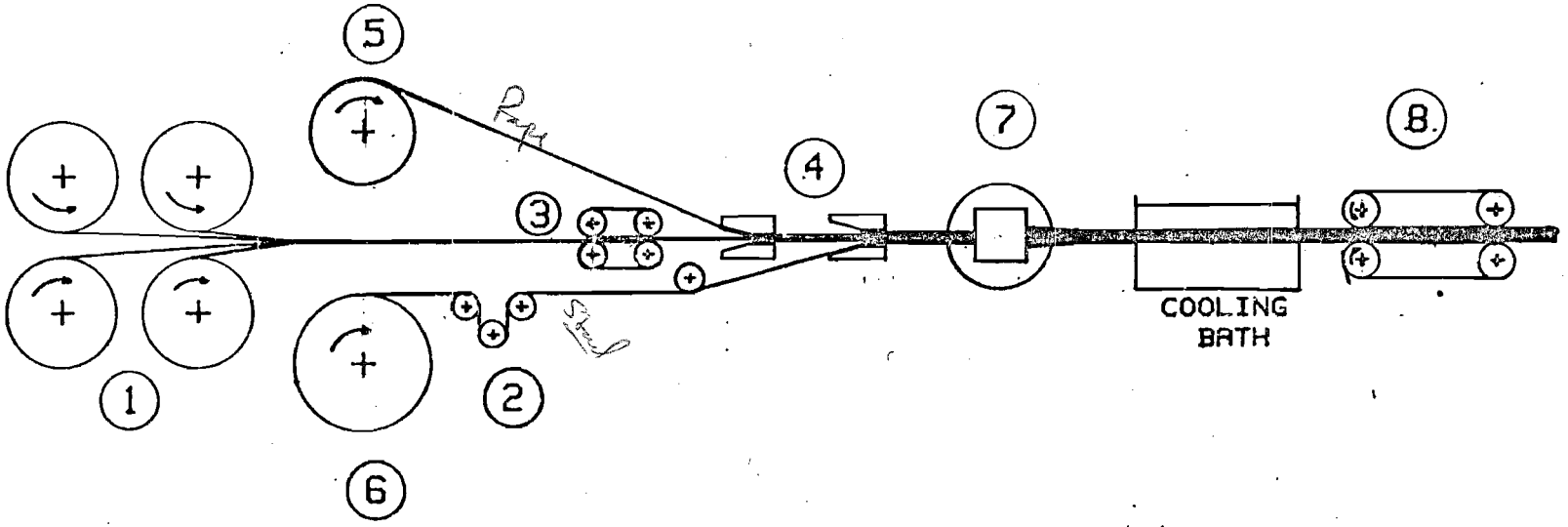

KEY:-

1. Fibre pay-off units
2. Line-speed sensor
3. Fibre haul-off unit
4. Tube forming head
5. Paper-tape pay-off
6. Steel-tape pay-off
7. Extruder crosshead
8. Caterpillar haul-off unit

DINORWIC PROJECT: CABLE MANUFACTURING LINE

FIGURE 6.8

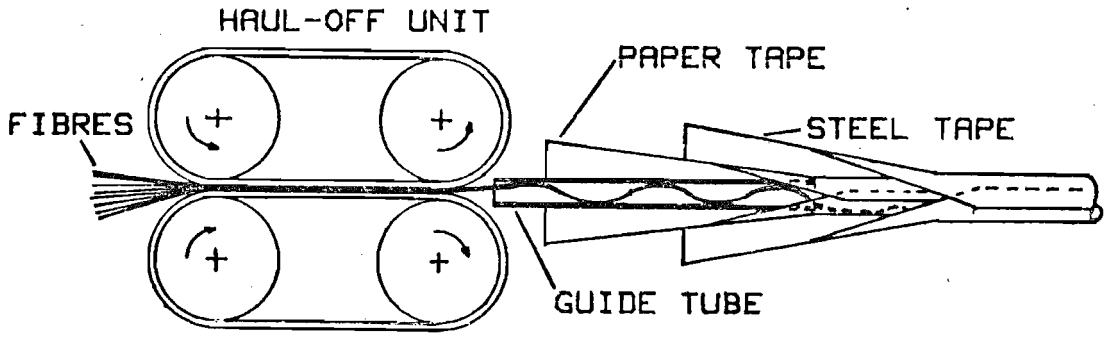

SCHEMATIC ILLUSTRATION OF HAUL-OFF AND GUIDE-TUBE FOR DRIVING FIBRES INTO LOOSE-TUBE CABLE.

FIGURE 6.9

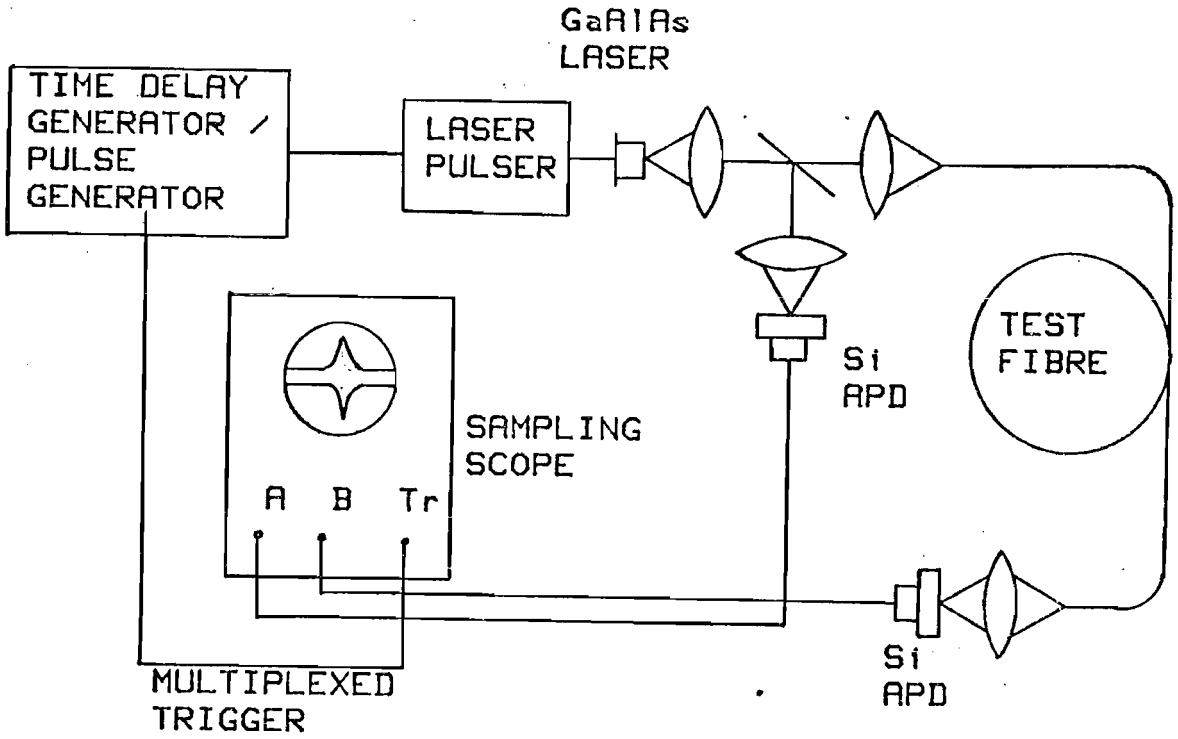

SCHEMATIC DIAGRAM OF PULSE TRANSIT-TIME MEASUREMENT SYSTEM.

FIGURE 6.10

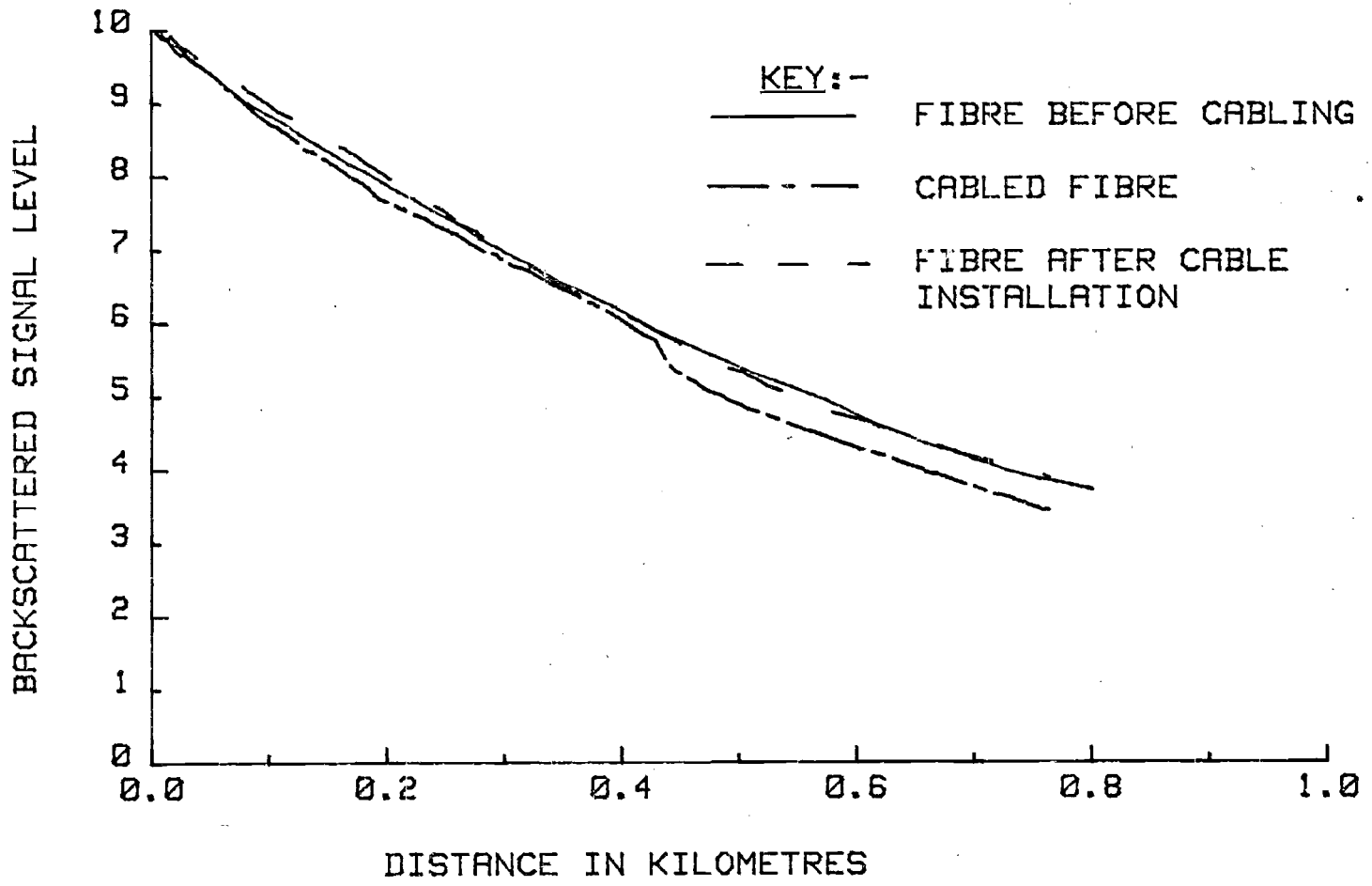

BACKSCATTER PLOTS OF FIBRE AT DIFFERENT STAGES OF CABLING.
The local increase of attenuation at ~425m is due to buckling of the fibre within the cable; the fibre excess length was greater than 1%.

FIGURE 6.11

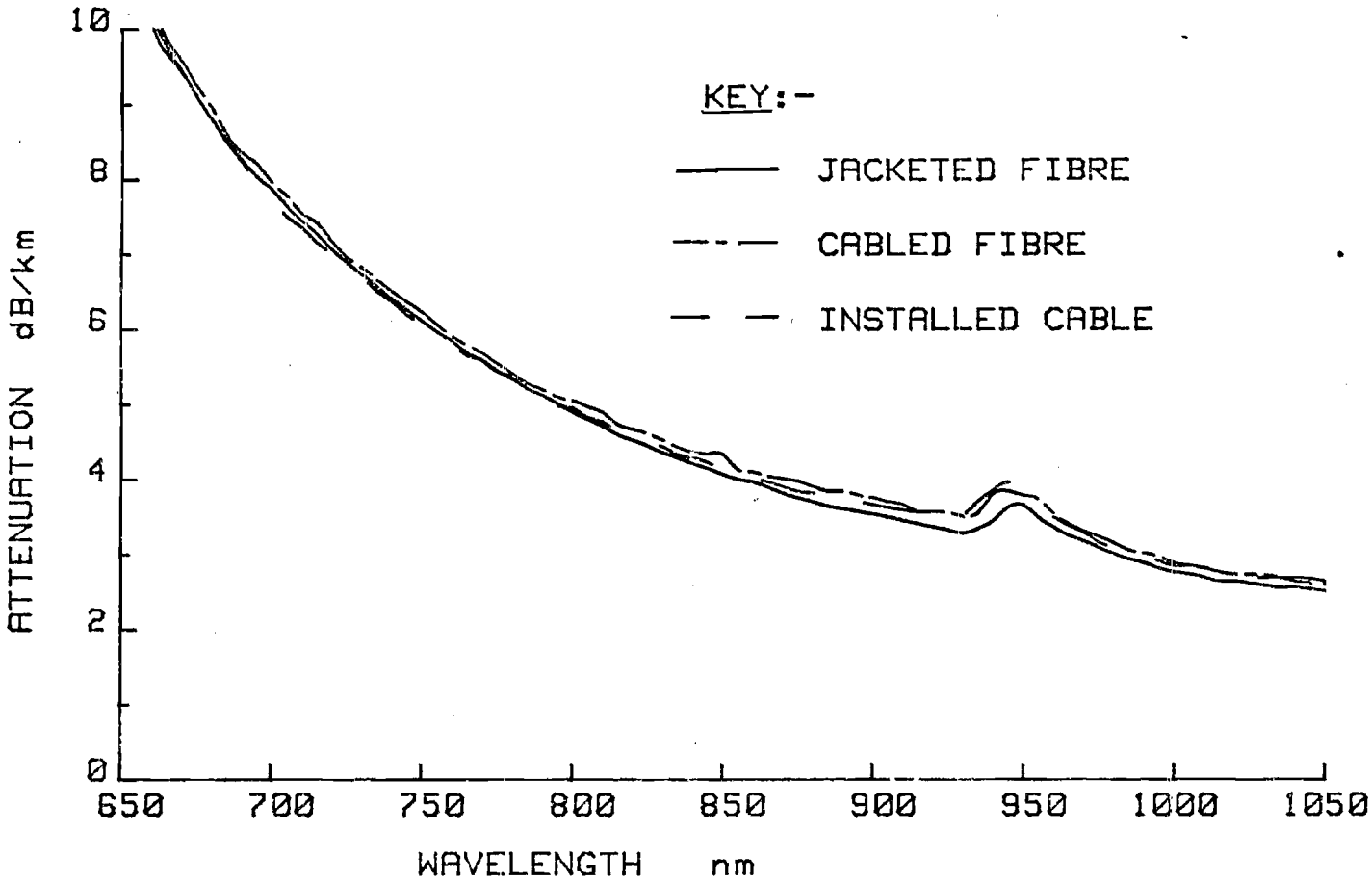

CHANGE OF SPECTRAL ATTENUATION DURING DINORWIC CABLE MANUFACTURE AND INSTALLATION

The measurements were made on a 1.25km length of cable in which the fibre excess length was ~0.5%

FIGURE 6.12

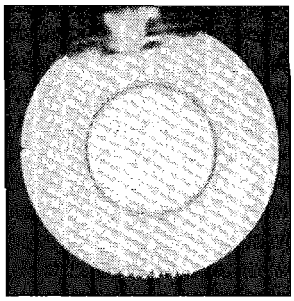

VD235

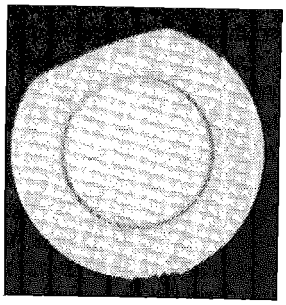

VD244

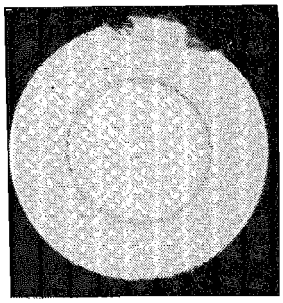

VD251

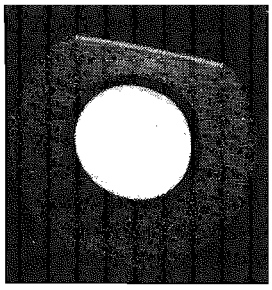

VD264

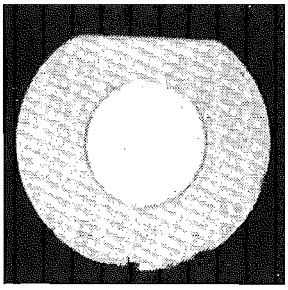

VD266

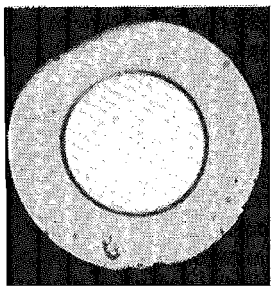

VD269

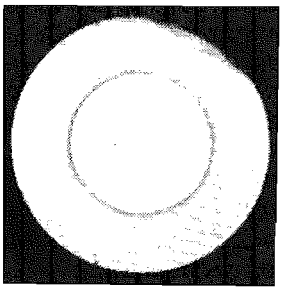

VD255

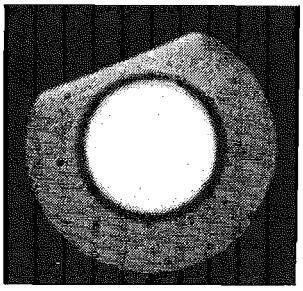

VD272

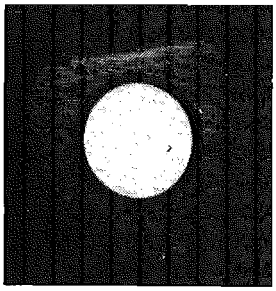

VD281

TRANSVERSE CROSS-SECTIONS OF THE GRADED-INDEX FIBRES USED IN THE DINORWIC OPTICAL FIBRE LINK.

FIGURE 6.13

A. LINEAR PLOT

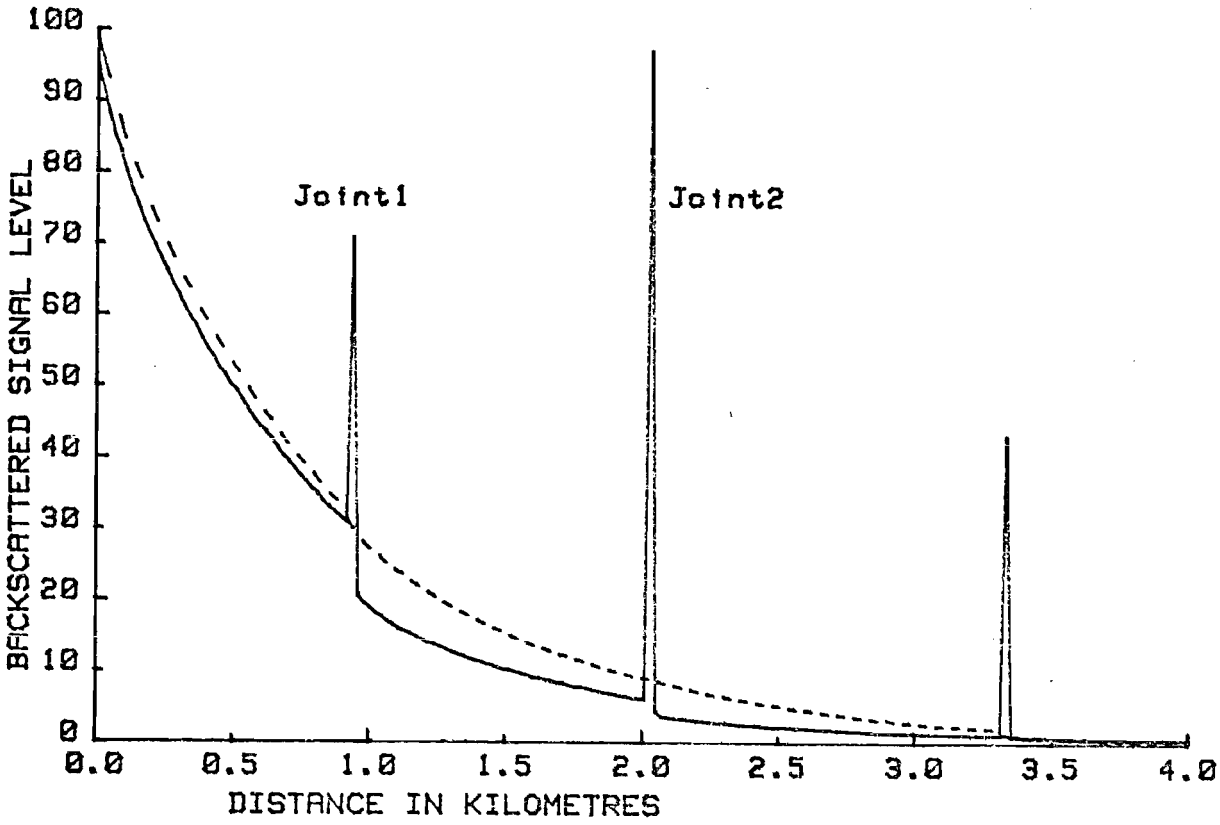

B. LOGARITHMIC PLOT

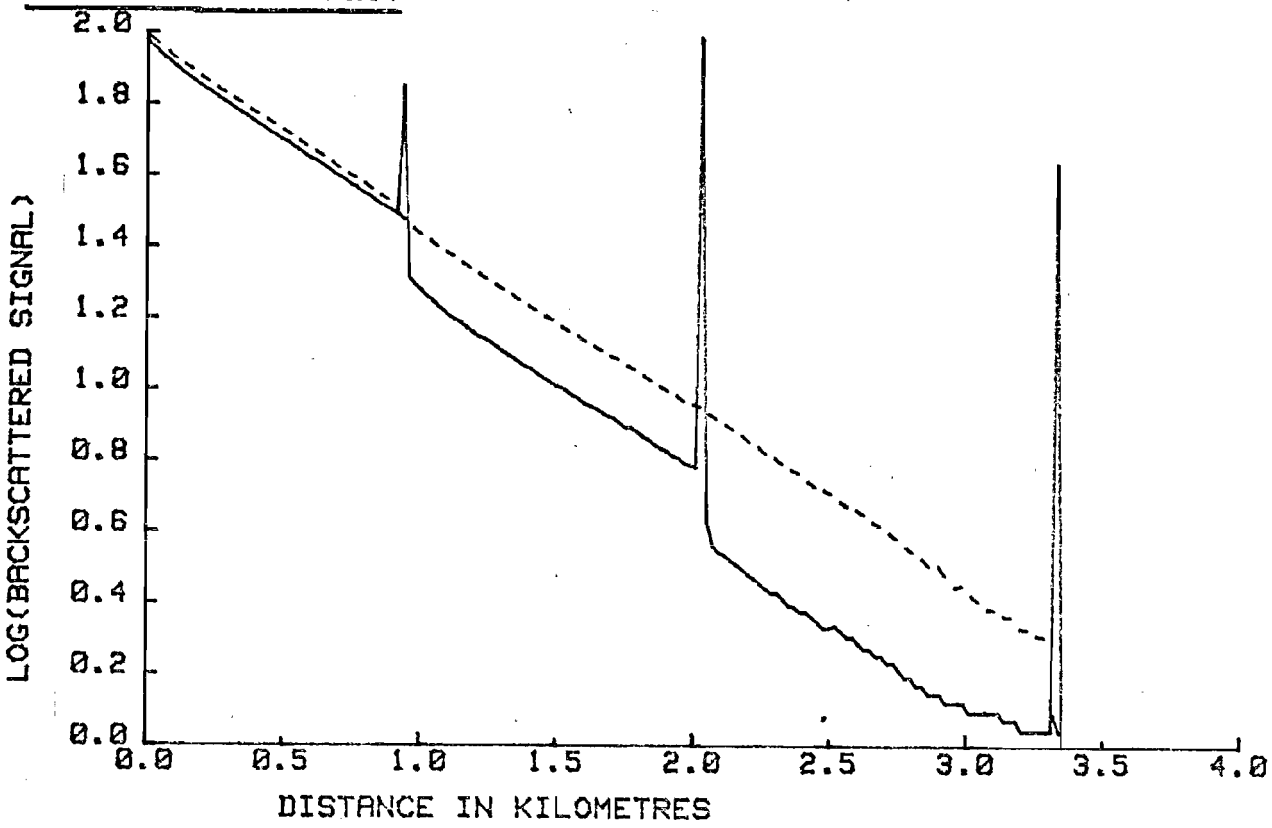

KEY:- ——— = V-GROOVE SPLICED ; - - - - - - = FUSION SPLICED

DINORWIC PROJECT: BACKSCATTER PLOTS OVER SECTIONS 1 TO 3 OF CHANNEL 1 WITH V-GROOVE JOINTS AND FUSION-SPLICED JOINTS.

FIGURE 6.14

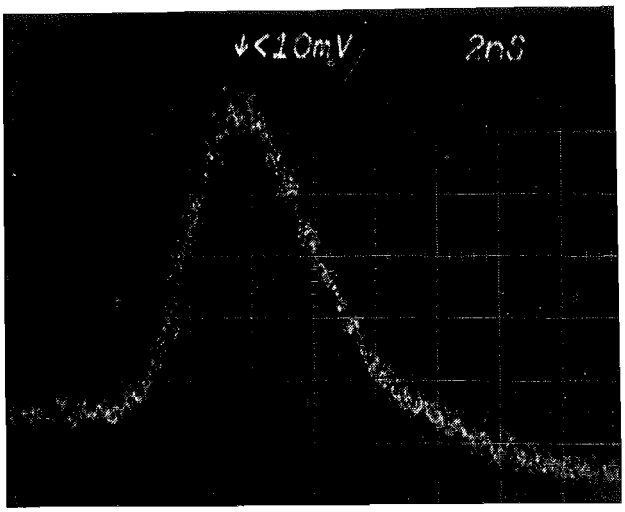

CHANNEL 1 O/P
4.3ns FWHM

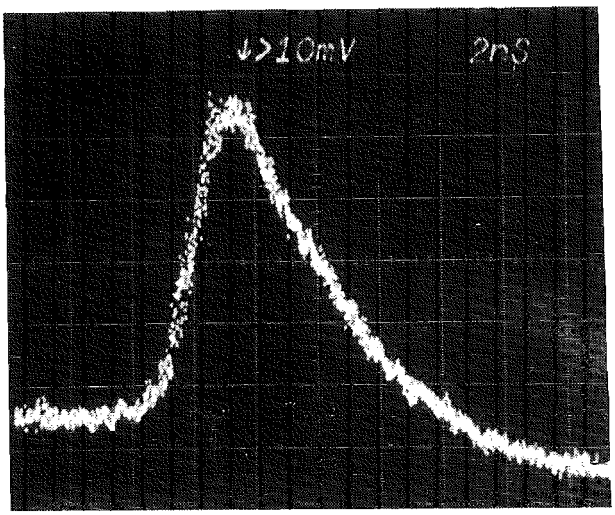

CHANNEL 2 O/P
4.2ns FWHM

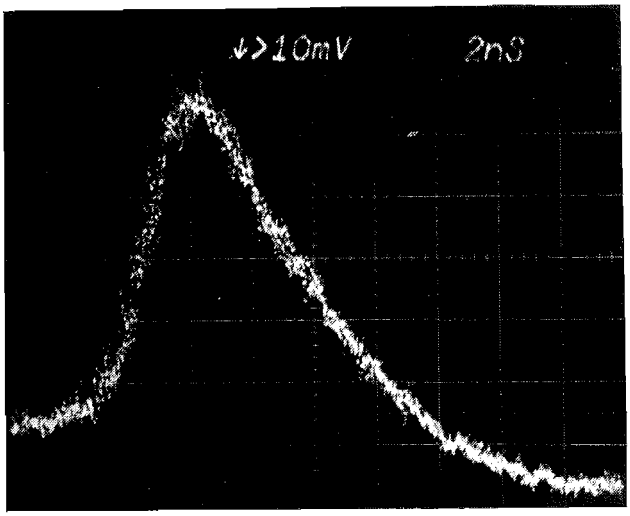

CHANNEL 3 O/P
5.0ns FWHM

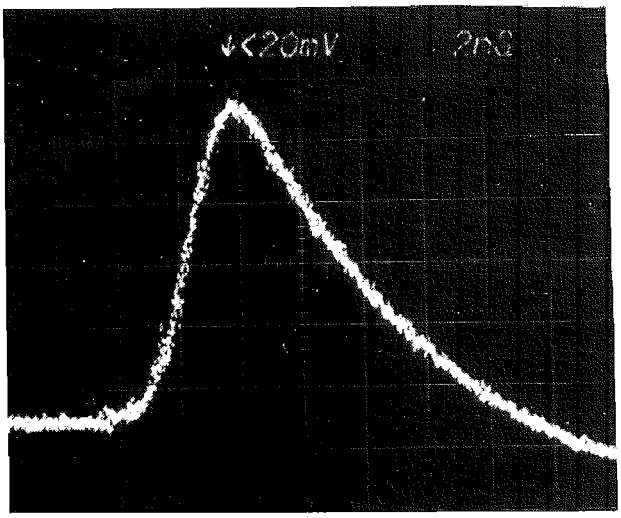

CHANNEL 4 O/P
5.3ns FWHM

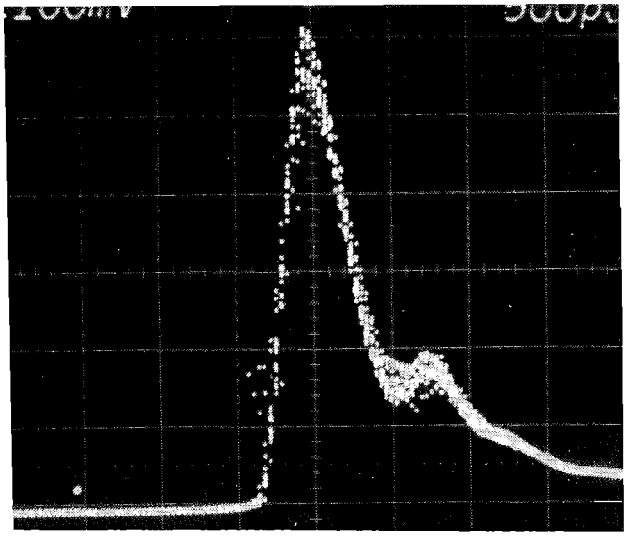

INPUT PULSE ; 0.5ns FWHM

DINORWIC PROJECT: PULSE DISPERSION OVER 5.3km LINK.
Measurement wavelength = 850nm ; laser linewidth ~ 2nm

FIGURE 6.15

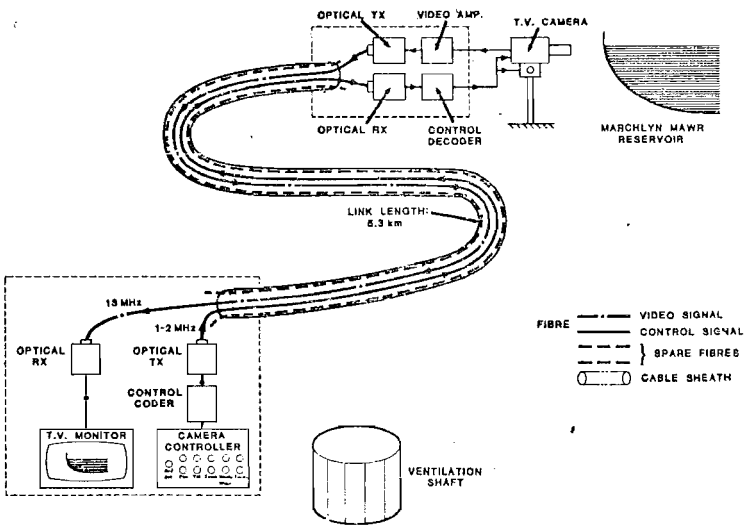

DINORWIC PROJECT: SCHEMATIC ILLUSTRATION OF VIDEO AND TELE-CONTROL OPTICAL FIBRE LINK.

FIGURE 6.16

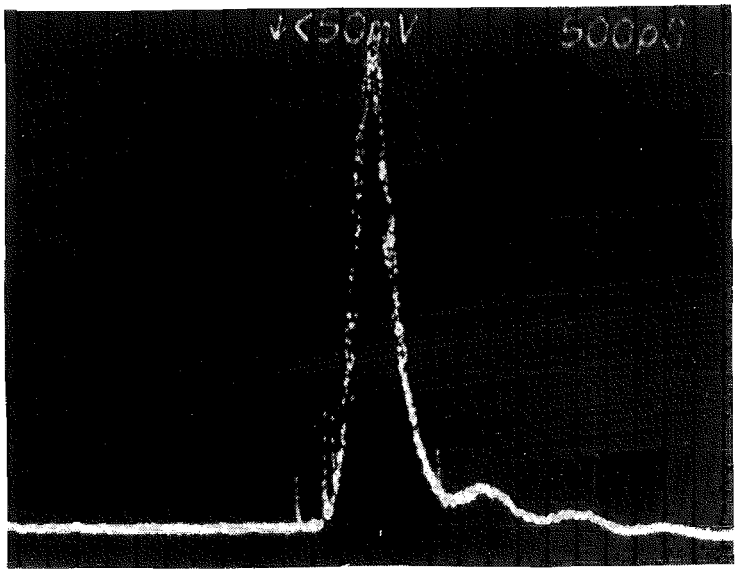

INPUT PULSE WAVEFORM
Pulsewidth = 300ps FWHM
Measurement wavelength = 843nm
Laser linewidth ~ 2nm

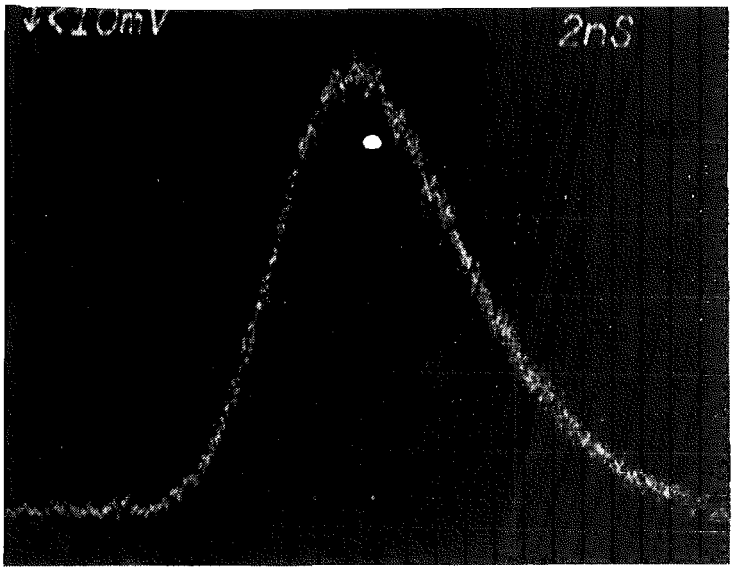

OUTPUT PULSE WAVEFORM
Pulsewidth = 5.8ns FWHM

FWHM PULSE DISPERSION = 5.8ns OVER 6.6km

0.878 ns/km

DINORWIC PROJECT: 34Mb/s TRIAL; PULSE DISPERSION OVER 6.6km LINK

FIGURE 6.17

DINORWIC PROJECT: 34Mb/s SYSTEM TRIAL

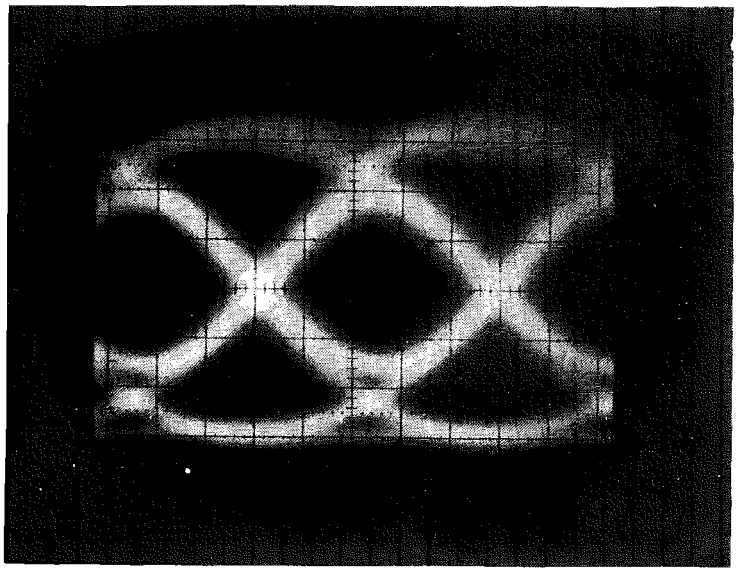

EYE-DIAGRAM AT DETECTOR OUTPUT
Timebase = 5ns/div
The eye-diagram was measured at the detector output after signal transmission over 6.6km of fibre.

Source: High-radiance LED operating at 904nm
Source Linewidth ~ 40nm

Detector: Silicon avalanche photodiode
Detector risetime < 100ps

Measured line attenuation = 22.5dB at 904nm

System bit-error-rate [BER] < 1 x 10-10

FIGURE 6.18

CHAPTER 7: CONCLUSIONS

The work presented in this thesis has resulted in the practical realisation of an optical communications system employing graded-index optical fibres manufactured by the homogeneous chemical vapour deposition process. The work has concentrated on the practical aspects of fibre manufacture, protection and cabling, and has led to significant advances in many areas ranging from glass preparation to cable design and production. In particular, techniques have been developed for the manufacture of high-quality fibres by HCVD, and the development of fibre-coating processes has enabled the fibres to be cabled without deterioration of their optical and physical characteristics.

7.1 Fibre Manufacture

7.1.1 Fabrication of Preforms by HCVD

The investigation of the glass systems which can be produced by HCVD has revealed that the binary phosphosilicate and germanosilicate glasses each possess processing characteristics which make it difficult to obtain reliably good geometry and accurately-controlled refractive index profiles in multimode fibres. The development of multimode fibres having a phospho-germanosilicate core-glass was a major contribution of this study. The ternary glass offers many advantages over the binary core-glasses, especially in terms of the thermal and physical properties which govern the processing characteristics of the material. These advantages have subsequently been recognised in other laboratories, and the ternary glass is now in general use for the manufacture of high-quality multimode fibres.

The development of an HCVD system, as described in Chapter 2, employing a modified glass-working lathe and a programmable reactant-distribution system has led to major improvements in the control of the deposition and collapsing processes. Using this equipment and the phospho-germanosilicate glass system it has been possible to manufacture preforms capable of yielding long lengths of high-quality fibre. The versatility of the HCVD process allows great freedom in the selection of the preform characteristics, and the techniques developed here allow preforms for multimode graded-index, multimode step-index and monomode fibres to be routinely produced. By careful engineering of the manufacturing techniques, the present work has not only resulted in an improvement in the quality of the preforms, but has also brought about a significant increase in the glass deposition rate, thereby making the process more economic for use in a production environment.

7.1.2 Drawing of Fibres from HCVD Preforms

At the outset of this study it was expected that the drawing of fibres from HCVD preforms would pose few problems, and that the stability of the drawing process would yield near-perfect fibres of constant diameter. However, the incorporation of fibre-diameter measurement into the fibre-drawing process has revealed that this is not the case, and a number of sources of fibre diameter fluctuations have been identified. Although modifications to the preform manufacturing process and to the design of the high-temperature, fibre-drawing furnace have significantly reduced the diameter variations, it has been necessary to introduce feed-back control of fibre diameter to eliminate long-term diameter variations due to preform taper. Using diameter control it is now possible to draw 125 μm fibre with less than 1 μm diameter variation over lengths in excess of 4 km. In some cases lengths of graded-index fibre in excess of 5 km have been drawn, and by preform-sleeving there is potential for even longer lengths to be obtained, particularly in the case of single-mode fibres.

7.1.3 The HCVD Process - Recommendations for Future Work

The HCVD process is essentially a batch process involving the manufacture of discrete quantities of material (the preforms). Obviously there are differences in quality from preform to preform, and the optical characteristics of the resultant fibres will be expected to differ also. In a manufacturing environment this will invariably lead to the introduction of a selection process whereby the fibres are graded according to criteria such as loss, bandwidth and geometry; selection on this scale is not only inconvenient but is also costly. The preform-scanning technique provides a means for characterising the preform and can thus yield valuable information for optimising the HCVD process. It is therefore suggested that considerable benefit might be gained from an 'iterative' optimisation of the preform-manufacturing process, involving feedback of information gained from preform-scanning to adjust the parameters of the HCVD process and to converge on an improved preform design. In this manner it should be possible to further reduce the distribution of performance from fibre to fibre.

On a more fundamental note, the HCVD process is still very much a 'black art' which, although it can be accurately controlled, is not fully understood. Specific examples are the reaction mechanisms which determine the dopant incorporation ratio, and the mechanisms which lead to the non-uniform refractive index profile across each deposition layer. Although these effects may have been noted, they have generally been 'put aside' in the drive for the development of low-loss fibres. It is suggested that now may be an opportune time to look back at the fundamentals of the deposition process in order to investigate in greater depth the parameters which affect the characteristics of the deposited glass.

Finally, the HCVD technique provides a high-purity reaction environment in which ultra-pure glasses can be prepared; by employing high-purity starting chemicals it has been shown that transition metal impurities in the glass can be reduced to insignificant levels.

Accordingly, as shown in Chapter 4, it is possible to fabricate graded-index, multimode fibres in which the attenuation over the 0.7μm to 1.2 μm region approaches the intrinsic limit for the core-glass. However, the advantages that can be obtained by operating optical fibre systems at longer wavelengths (1.3 μm or 1.55 μm) have placed great emphasis upon the need to minimise the absorption losses due to the presence of hydroxyl ions within the waveguide glasses. The deposition system described in this thesis was designed in 1977 with the prime objective of developing low-loss fibres for use in the 0.85 μm region; although the significance of hydroxyl absorption was appreciated, it was considered to be of secondary importance to the elimination of transition metal impurities, and, apart from using molecular sieves to dry the carrier gases and ensuring that the deposition system was gas-tight, no specific actions were taken to eliminate hydrogen-containing species in the reactant chemicals. However, workers in the U.S.A. have recently identified the hydrogen-containing species as a major source of hydroxyl contamination in the deposited glass, and by using chlorine to getter the hydrogen as HCl (both in the reactant liquids and also during the deposition and collapse processes), have been able to greatly reduce the hydroxyl absorption losses. It is therefore suggested that a further improvement in the quality of our preforms could be obtained by using similar techniques to ensure that the hydroxyl impurity level is acceptably low.

7.2 Transmission Characteristics of HCVD Fibres

7.2.1 Multimode Fibres

Prior to the inception of this study, it had been demonstrated that the HCVD process could provide multimode fibres having low attenuation in the wavelength region of interest to optical communications. At the commencement of the study, it was possible, with care, to manufacture fibres having minimum losses of the order of 3 dB/km in lengths of about 1 km. The deposition equipment was rudimentary and process control was such that it was difficult to guarantee other important parameters such as core size, numerical aperture, refractive index profile and bandwidth.

In contrast, the development of the HCVD system and the phospho-germanosilicate glasses, as described in Chapter 2, has brought about major improvements in the geometrical and optical properties of the fibres; hence, on completion of the experimental-study period in 1978, it was possible to achieve less than 1 dB/km loss in multimode, graded-index fibres having lengths in excess of 5 km.

Comparison of the spectral loss characteristics of phosphosilicate- and phospho-germanosilicate-cored fibres shows that the Rayleigh scattering loss is higher in the latter case, and that in the 0.85μm region a loss penalty of about 1 dB/km may be incurred if the ternary glass is used. Nevertheless, as is shown in Chapter 4, this disadvantage is more than offset by the overall performance characteristics of the phospho-germanosilicate fibres: Using the ternary glass system, numerical apertures of 0.25 are readily attained, and accurate control of the refractive index profile can be achieved. Furthermore, at wavelengths beyond 1 μm the reduced Rayleigh scattering loss has enabled attenuation as low as 0.8 dB/km to be obtained in a fully-excited length of fibre. In addition, a "standard" graded-index fibre has been developed, and, as a consequence of the profile control, very high bandwidth capabilities have been measured. Although the primary objective of the fibre-manufacturing programme was to develop low-loss fibres for use in the 0.85 μm region, spectral attenuation measurements have shown that the fibres are well suited to operation in the 1.3 μm and 1.55 μm regions provided that care is taken to maintain the OH impurity contamination of the core-glass at an acceptable level.

The assessment of the optical characteristics of a sample of twenty "standard" graded-index fibres revealed a narrow performance distribution. Although many of the fibres were drawn without feedback control of fibre diameter, the extreme values of the attenuation distribution differed by only 1.5 dB/km. Similarly pulse dispersion measurements gave a narrow spectrum of results; in all cases the intermodal dispersion did not exceed 2.5 ns/km and in some cases was as low as 0.3 ns/km.

The variation of pulse dispersion from fibre to fibre is attributed to the sensitivity of the bandwidth to small-scale perturbations of the ideal refractive index profile. Nonetheless, on an optimistic note, the distribution of performance in these fibres is somewhat better than is found in similar fibres which are manufactured on a commercial basis by Corning Glass Works. Furthermore, the impressive results of this performance study led to the transfer of the fibre-manufacturing technology to industry where the same techniques are being employed to manufacture fibres for the telecommunications market.

7.2.2 Single-mode Fibres

Single-mode fibres offer the advantage of very high bandwidth due to the absence of intermodal dispersion. During the course of this study it has been shown that the HCVD process can be applied to the manufacture of single-mode fibres, and that low attenuation levels can be achieved. The attenuation level of the monomode fibres is marginally higher than is obtained in multimode fibres, and by reducing the waveguide losses a further improvement is certainly possible. Spectral attenuation measurements over the 0.7 μm to 1.7 μm region have shown the importance of attaining low OH levels in fibres which are to operate in the 1.3 μm and 1.55 μm regions; a reduction of the hydroxyl level present in our fibres must be achieved if ultra-low attenuation is desired at 1.3 μm.

A convenient technique for determining the normalised frequency, core diameter, and core/cladding index difference of monomode fibres has been developed at Southampton. The technique, which involves measurement of the power distribution in the far-field radiation pattern of the fibre under test, has been employed to characterise monomode fibres made during the course of this study; it has been confirmed that the method is both accurate and convenient. Furthermore, it has been shown that an alternative method for estimating the normalised frequency is prone to considerable inaccuracy, and is unable to yield data on the core size and index difference.

The current interest in monomode fibres stems not only from optical communications but also from their potential for use in instrumentation, where their ability to transmit coherent polarised light is most attractive. In one application the Faraday rotation of polarised light propagating in a monomode fibre is used to determine the electrical current passing through a conductor. As the sensitivity of this device is limited by residual birefringence of the fibre, a systematic study of the causes of the birefringence has been undertaken. Both core ellipticity and anisotropic stress within the fibre were found to have a dramatic influence upon the birefringence. A number of fibres were manufactured to gain an insight into these effects, and a novel design was conceived for a monomode fibre in which the stress-induced birefringence would be considerably reduced. A fibre was manufactured to this design, and was found to exhibit the spectacularly-low linear birefringence of 2.6°/m. This result represented a major advance when it was achieved in 1977, and still represents the lowest reported figure for the birefringence in any monomode fibre. The fibre was also found to be insensitive to the effects of vibration, temperature and microbending, and was subsequently installed in a current-sensing transducer which has been successfully operated for over two years in the CEGB power-generating station at Fawley, Hampshire.

7.3 Protective Coatings

7.3.1 Primary Coatings

When this research programme was undertaken in 1975, it was realised that although it was possible to handle bare fibres without breakage in the research laboratory, to achieve widespread utilisation in the field, it would be necessary to improve the strength performance of the fibres under tensile loads. It was also recognised that freshly-drawn glass fibres could exhibit considerable strength, which was severely degraded by the introduction of surface flaws under mechanical abrasion or atmospheric attack. An original programme of of work was therefore initiated with the objective of maintaining the high inherent strength of freshly-drawn optical fibres by the application of a surface protective coating in-line with fibre drawing.

The work has involved an assessment of potential coating materials, design of novel equipment for the application of the coating, and has resulted in the development of a coating which produces a considerable improvement in fibre strength.

Contrary to expectations it was found that the physical characteristics of the coating material were not of the utmost importance in determining the strength characteristics of the coated fibre. The most critical factor proved to be the method of application and the processing characteristics of the coating materials. Although polyorganosiloxanes offer excellent physical properties in the cured state, the application of the partially-polymerised materials from a solvent solution proved troublesome. On the other hand, it was found that thermosetting silicone elastomers are easily applied from a solventless liquid, and can be applied and cured in thick sections. The elastomers have a very low modulus, low tensile strength and do not bond to the silica fibre surface yet produce a considerable improvement in fibre strength. Thus a median tensile strength of 5.2 GN/m^2 was measured in 1.0 metre gauge-length samples, and a mean breaking load in excess of 60 N was achieved; this represents an improvement of more than an order of magnitude over the strength of bare fibre samples which have been subjected to normal handling procedures. The silicone coating does not degrade the optical performance of graded-index fibres, and its low modulus is advantageous in providing a degree of buffering against microbending forces. Indeed, the attractions of the silicone primary coatings are such that they have been independently developed in other laboratories, and are probably the most common primary coating currently in use.

7.3.2 Secondary Coatings

A hard outer secondary coating of an extruded thermoplastic not only improves the microbending resistance of the primary-coated optical fibres, but also protects the soft, silicone primary coating from abrasion during handling and cabling procedures. An experimental evaluation of materials suitable for jacketing of silicone-coated fibres has been undertaken, and an extrusion line has been designed and commissioned exclusively for use with fibres.

In contrast to the experiences with primary coatings, it was found that the physical properties of the secondary coating were of crucial importance in determining the performance of the jacketed fibre. Experimental trials verified initial predictions that, in comparison with other common thermoplastic coating materials, nylon 6 possesses the most attractive physical characteristics. It has also been established that the cooling and crystallisation of the extrudate have a strong influence upon the optical performance of the fibres at low temperatures. By suitable control of the extrusion conditions the excess loss introduced by jacketing was reduced to negligible levels over the temperature range -40°C to 60°C. Similarly by controlling the crystallisation of the extrudate, it has been possible to overcome the problems of colour-coding the jacket and to increase its thickness without degrading the optical performance of the standard graded-index fibres.

The combination of a silicone rubber primary coating and a nylon 6 outer jacket thus offers an excellent degree of protection from the effects of lateral forces and axial tensile loads without degrading the high performance characteristics of the phospho-germanosilicate graded-index fibres. Though this composite, jacketed-fibre configuration is similar to designs which have been developed elsewhere, the use of nylon 6 as the hard outer shell is novel. By virtue of its high elastic modulus, the nylon 6 jacket provides superior protection against tensile loads and microbending forces, and is therefore a significant improvement to the 'state of the art'.

7.3.3 Protective Coatings - Recommendations for Future Work

The work on primary coatings has demonstrated the high inherent strength of HCVD fibres, and has shown that silicone elastomers provide sufficient protection of the fibre surface. Preliminary work on flaw characterisation has shown that two classes of flaw are present, thus producing a bimodal Weibull strength distribution. The first class of flaw is characterised by a narrow distribution of very high fibre strengths, whilst the second type of flaw produces a broader distribution of marginally lower strength.

The tensile strength of long lengths of fibre, determined by the second class of flaws, is by no means restrictive, and it has been shown, both theoretically and practically, that the fibre strength is more than sufficient to withstand the tensile loads experienced in cabling. Nevertheless, it is suggested that by suitable modification of the fibre-drawing and preform-manufacturing processes it may be possible to obtain a further improvement in the distribution of flaw sizes, thereby attaining an overall improvement in the strength of very long lengths of fibre.

Although initial experiments have indicated that the transmission characteristics of the low-loss monomode fibres are unaffected by the application of a jacket, there remains considerable scope for evaluating the effects of jacketing upon loss, microbending performance, and even birefringence in monomode fibres.

7.4 Optical Fibre Field Trial at Dinorwic

The Dinorwic project presented the ideal opportunity to evaluate the performance of HCVD fibres in an operational optical communication system. The severity of the cable route and the site conditions also offered a challenge to the cable manufacturer and installers, and dictated the need for a cable which is both rugged and flexible. The final cable design satisfied these requirements and can be put into production in a single operation. Using a novel technique to drive an excess length of fibre into the cable structure an additional safety margin against fibre breakage during installation has been obtained.

The results of the fibre and cable manufacture, and of the subsequent installation were an unqualified success. The graded-index fibres exhibited very good attenuation and pulse dispersion characteristics, neither of which were significantly affected by the jacketing, cabling and installation operations. The importance of low-loss joints was clearly demonstrated when the V-groove joints were replaced with splices made by the arc-fusion method. Measurements on the four-channel, 5.3km link revealed that at 0.85 μm the mean attenuation of the jointed link was 3.77 dB/km, only 0.1 dB/km above the level of the jacketed fibres before cabling; using a laser source operating at 0.85 μm, in all cases the combined effects of intermodal and material dispersion amounted to less than 1 ns/km pulse broadening.

The performance of the optical cable was well within the limit laid down in the system specification, and the video link performed satisfactorily even when an additional loss of 10 dB was introduced! The subsequent installation, in 1980, of the 34 Mb/s optical line system further emphasised the capabilities of the phospho-germanosilicate graded-index fibre: Even though the use of an LED source resulted in a low launched power and considerable material dispersion, the system performance over a 6.6 km link gave a BER of less than 1×10^{-10}. Although the system is at present transmitting pseudo-random data, it does represent the first installed and operational 34 Mb/s optical communications system within the U.K., and will probably become part of the C.E.G.B.'s communications network at a later date.

7.5 Concluding Remarks

In summary, it is felt that the present study has made a significant contribution to the development of low-loss optical fibres for telecommunication. The work has resulted in the development of the ternary phosphogermanosilicate glasses for use in multimode fibres, and has involved the design and development of a lathe-based HCVD system. The versatility of the process allows high-quality preforms for multimode graded-index, multimode step-index, and monomode fibres to be routinely manufactured.

The incorporation of fibre-diameter measurement equipment into the fibre-drawing line led to the identification of a number of fibre-diameter noise sources; optimisation of the preform-manufacturing and fibre-drawing processes has brought about a considerable improvement in the fibre performance. On completion of the project it is possible to draw very long lengths of multimode fibre having accurately-controlled diameter, geometrical configuration and refractive index profile, with attenuation levels approaching the fundamental limit for the core glass.

Perhaps the most outstanding feature of the development work on monomode fibres is the major advance made in the fabrication of fibres possessing very low birefringence.

Much of the research programme has been concerned with the practical application of optical fibres within a field environment. Thus, the development of primary coatings for the preservation of fibre strength was of great importance, and led to the development of effective coating techniques. Moreover, the subsequent extension of this work to include the application of a tough secondary coating was of comparable importance for the successful application of HCVD fibres; although the concept of applying a secondary coating to improve the mechanical protection and microbending resistance of fibres is well-established, the use of nylon 6 as the jacketing material is novel, and has been shown to offer superior performance both in terms of the optical and physical characteristics of the jacketed fibre.

The Dinorwic project provided the ideal opportunity to illustrate the capabilities of the fibres developed during this study. The severity of the installation environment was reflected in the design of the optical fibre cable, and the author's involvement with the cable manufacture culminated in the development of a novel cabling technology, for which patents have been filed in more than fifteen countries. The initial specification for the performance requirements of the optical link was proven to be overcautious when the link was installed. Such is the success of the installation that the video link is to become a vital part of the security system at Dinorwic, and the 34 Mb/s line system is likely to become an integral part of the CEGB communications network.

CHAPTER 8: ACKNOWLEDGEMENTS

There are many colleagues who deserve acknowledgement for the advice, assistance and encouragement which they have given during the course of this study.

In the Optical Communications Group at the University of Southampton I would like to thank Dr. D.N. Payne for his guidance and many useful ideas. Other members of the group who have contributed directly to the work are Dr. C.R. Hammond, Dr. F.M.E. Sladen, Mr. A.H. Hartog, Dr. H. Matsumura, Mr. I. Sasaki and Dr. M.J. Adams. To these and all other members of the group, including the workshop staff and Mrs. J. Ditchfield, I express my sincere thanks for the part they have played in transforming a lowly mechanical engineer into the master of a new technology!

I am deeply indebted to Prof. W.A. Gambling for supervising the work, for his persistence in encouraging me to write this thesis, and for his constructive comments on the manuscript.

At the Pirelli General Cable Works I must thank my colleagues in the Optical Fibre Group for their assistance in the experimental programme. In particular I must thank Mr. P.L. Scrivener, Mr. S.A. Clayton and Mr. R.E. Collis for their collaboration on the Dinorwic Project. Grateful acknowledgement is also made to Dr. G. Maschio and Mr. J.R. Osterfield for their encouragement since my return to the Company. The efforts of Mrs. Freeman and her staff in typing the manuscript must be mentioned, as must Paul Scrivener's labours in proof-reading the typescript.

Finally, I am deeply indebted to the Pirelli General Cable Works Ltd.. and to the Science Research Council for the award of an Industrial Research Studentship.

CHAPTER 9: LIST OF PUBLICATIONS, CONFERENCE PAPERS AND PRIZES

The work presented in this thesis has resulted in a number of publications and conference papers which are listed in chronological order.

9.1 Publications

1. Gambling, W.A., Payne, D.N., Hammond, C.R., and Norman, S.R.: 'Optical fibres based on phosphosilicate glass'. Proc. IEE, 123 (1976), p.p. 570 - 576.

2. Gambling, W.A., Payne. D.N., Matsumura, H., and Norman, S.R.: 'Measurement of normalised frequency in single-mode optical fibres', Electron. Lett., 13 (1977), pp. 133 - 135.

3. Sladen, F.M.E., and Norman S.R.: 'Data transmission using optical fibres', Electronic Engineering, June 1977, pp. 57 - 63.

4. Hammond, C.R., and Norman, S.R.: 'Silica-based binary glass systems - refractive index behaviour and composition in optical fibres', Opt. Quant. Electron., 9 (1977), pp. 399 - 409.

5. Norman, S.R., Payne, D.N., Adams, M.J. and Smith, A.M.: Fabrication of single-mode fibres exhibiting extremely low polarisation birefringence, Electron. Lett., 15 (1979), pp. 309 - 311.

6. Norman, S.R.: 'Fabrication and evaluation of single-mode fibres', Phys. Chem. Glasses, 21 (1980), pp. 53 - 57.

9.2 Conference Papers

1. Norman, S.R.: 'The preparation of ultra-pure phosphosilicate glasses by chemical vapour deposition', Symposium on unusual methods of glass formation for inorganic and metallic systems'. Society of Glass Technology, Sheffield U.K., Jan. 1977.

2. Norman, S.R.: 'Single-mode fibres for current measurement', C.E.G.B. Symposium on Opto-Electronics, C.E.R.L., Leatherhead, U.K. Jan. 1978.

3. Norman, S.R.: 'Optical fibre fabrication', Symposium on new developments in line and radio transmission systems', I.B.A., Crawley, U.K., May 1978.

4. Norman, S.R., 'Evaluation of the properties of single-mode fibres', Colloquium on optical fibres, Society of Glass Technology, Imperial College, London, Jan. 1979.

5. Norman, S.R., Payne, D.N., Adams, M.J., and Smith,A.M.: 'Single-mode fibres exhibiting extremely low polarisation birefringence, 'Fifth European Conference on Optical Communications, Amsterdam, Sept. 1979.

6. Osterfield, J.R., Norman, S.R., McIntosh, D.N., Rogers, A.J., Castelli, R., and Tamburello, M.,: 'An optical fibre link in a mountainous environment', 29th International Wire and Cable Symposium, Cherry Hill, U.S.A., Nov. 1980.

9.3 Prizes

The Institution of Electrical Engineers awarded the Electronics Division Premium for 1976 jointly to Prof. W.A. Gambling, Dr. D.N. Payne, Dr. C.R. Hammond and myself for the paper 'Optical fibres based on phosphosilicate glass'. The award was shared with a group from the British Post Office Research Laboratories who were similarly awarded for the paper 'Preparation of sodium borosilicate glass fibre for optical communication'.

The Institution of Electrical Engineers awarded the Electronics Division Premium for 1978 jointly to Prof. W.A. Gambling, Dr. D.N. Payne, Dr. H. Matsumura, Miss C.R. Ragdale and myself for a series of papers on monomode fibres which were published in Electronics Letters.